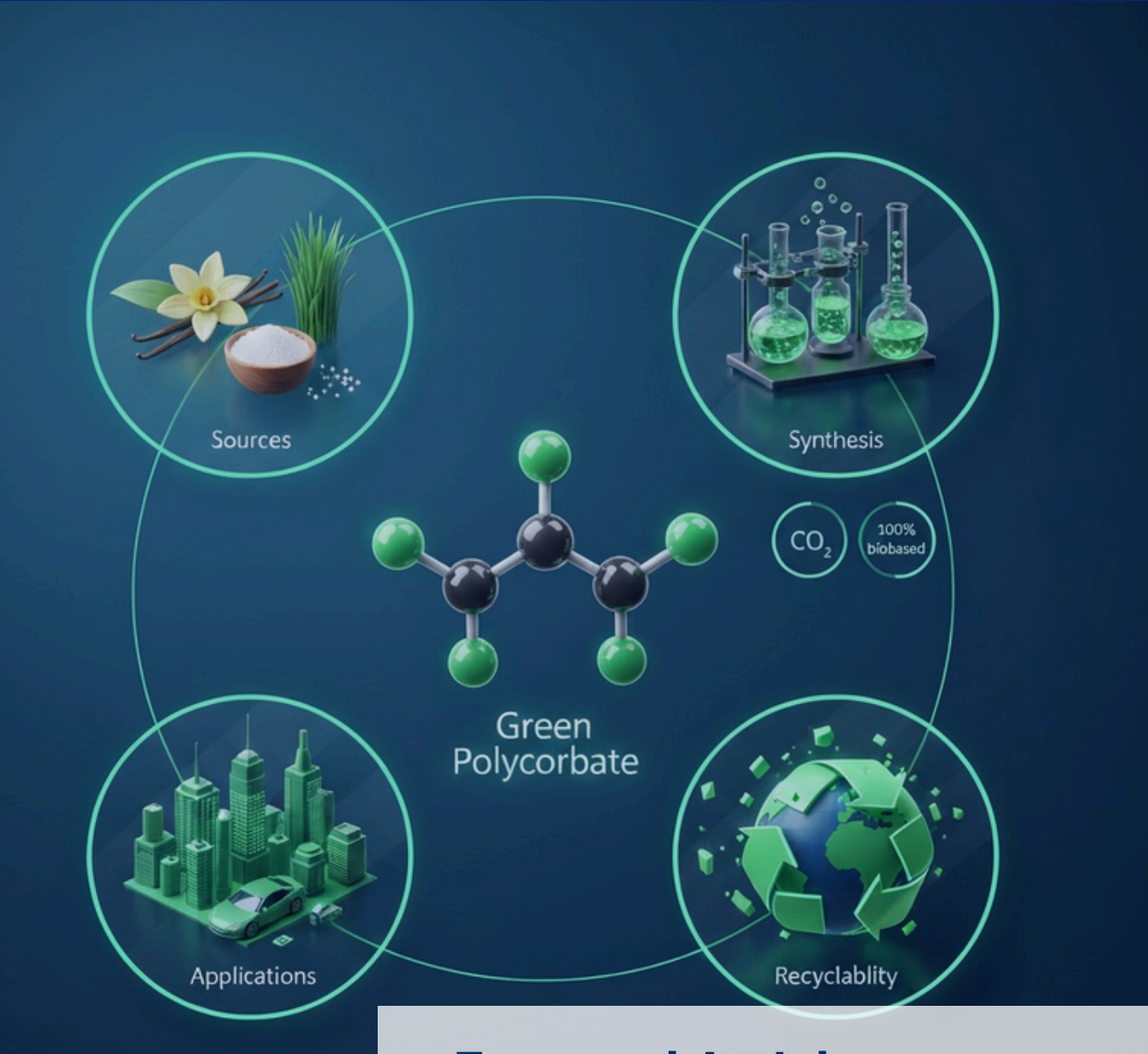
THE

JOURNAL OF CRIS



Featured Article

Recent Advances in Sustainable Polycarbonate Synthesis, Recyclability, and Emerging Applications

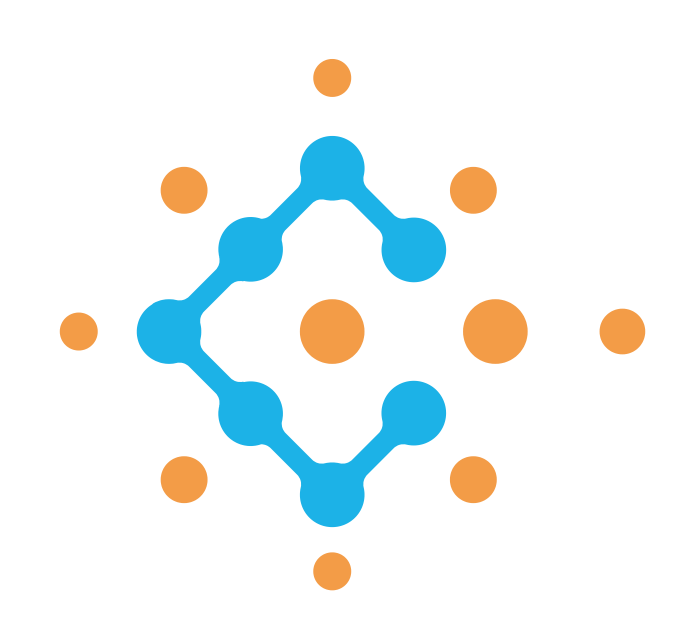


Table of **Contents**

02	Board Message	
03	Letter from the Editor	
04	New Approach to Produce Alumina Refractories from Waste Claus Catalyst Fatimah Edhaim, Sagar Patil, Ahmed Asseel	
11	Rietveld Quantitative Phase Analysis of XRD Data from Crystalline Deposits in Refinery and Gas Plant Equipment: Implications for Failure Diagnosis and Preventive Maintenance* Husin Sitepu, Rasha A. Al-Ghamdi, Mona S. Al-Dossary, and Husam S. Khanfar	
21	Integrative Characterization of Microbial-Induced Corrosion in Sulfur Recovery Unit Equipment Using Quantitative XRD and Rietveld Refinement Techniques Husam S. Khanfar, Husin Sitepu, Noha S. Alshihri, Mona S. Al-Dossary, Xiangyang Zhu and Ibrahim M. Al-Zahrani	
33	Recent Advances in Sustainable Polycarbonate Synthesis, Recyclability, and Emerging Applications Najd A. Alhussain, Florian Stadler	
44	Effect of UV Light on Some Mechanical Properties of Graphite Powder-Reinforced Polypropylene Developed for Roofing Application Shuaibu, M.A, Yusuf A., Jamilu, M.B., Mohammed A.B, Ali S M and Mustapha, A.	
57	Utilization of AggreBind's copolymer technology for landfill closure Alaa Abd Al Haq	
36	Editorial Board	
37	Success Partners	

Board **Message**

Dear Esteemed Readers,

It is with immense pride and excitement that I welcome you to the third issue of volume 2 of our society's technical journal. Building on the foundation laid in our inaugural issue, this edition signifies our unwavering commitment to fostering innovation, sharing knowledge, and strengthening connections within our professional community.

As our field continues to evolve, so too does the scope of ideas and challenges we face. This journal remains dedicated to providing a platform where groundbreaking research, practical insights, and diverse perspectives converge. It is our hope that these contributions spark dialogue, inspire action, and drive meaningful progress.

In this issue, you will find an enriched selection of articles that delve deeper into the complexities of our discipline. Each piece reflects the dedication and expertise of our contributors, as well as the collective vision of our society to lead and inspire. I encourage you to explore the content thoughtfully and consider how these insights might shape your work and broaden your understanding.

The success of this endeavor would not be possible without the support and collaboration of our authors, reviewers, and editorial team. Their hard work and passion have once again made this journal a testament to the vibrancy and depth of our community. As we move forward, let us continue to celebrate the spirit of curiosity, innovation, and excellence that unites us. Thank you for your ongoing engagement and support. Together, we are shaping the future of our field.

Warm regards,





Letter From The Editor

Dear Colleagues,

Welcome to the third issue of volume 2 of the Journal of Chemicals Research and Innovation Society. As we embark on another year of scientific exploration and knowledge sharing, we are excited to continue our mission of fostering groundbreaking research and collaboration in the chemical sciences.

Building on the foundation laid in our previous volumes, this issue presents a diverse collection of studies that showcase innovative methodologies, novel discoveries, and practical advancements across various fields of chemistry. Each contribution reflects the dedication and expertise of our research community, and we are proud to provide a platform for such impactful work.

I extend my deepest gratitude to our authors, reviewers, and editorial team for their unwavering commitment to excellence. Your contributions ensure that this journal remains a trusted source of scientific progress and a hub for meaningful discourse.

As we move forward, I encourage you to actively engage with the journal, whether through submitting your research, participating in discussions, or sharing insights with your peers. Together, we can continue to drive innovation and push the boundaries of chemical research.

Thank you for your continued support, and I look forward to the discoveries and advancements that lie ahead.

Best regards,

Shakeel Ahmed, Ph.D.,

Editor-in-Chief Journal of Chemicals Research and Innovation Society

New Approach to Produce Alumina Refractories from Waste Claus Catalyst

Fatimah Edhaim¹*, Sagar Patil², Ahmed Asseel¹
1 Research and Development Center, Dhahran, Kingdom of Saudi Arabia
2 Consulting Services Department, Dhahran, Kingdom of Saudi Arabia

*Corresponding author; email: fatimah.edhaim@aramco.com

Abstarct

A novel approach has been developed to produce high alumina refractory bricks by partially substituting bauxite with spent Claus catalyst, a waste product from gas processing plants. This method addresses waste disposal and reduces environmental impact. The synthesized bricks, composed of over 70% Al2O3, exhibited excellent thermal stability and cold crush strength, ranging from 1784 to 2654 psi. This surpasses some commercial alumina bricks. categorizing them as type 4 insulating refractory bricks. These materials can be used in fired heaters, boiler stacks, or fired heater convection sections. The study provides a solution for waste catalyst disposal while producing high-quality refractory bricks, offering a promising alternative to traditional methods. The results demonstrate the potential for sustainable and environmentally friendly production of refractory bricks, reducing and minimizing environmental waste footprint. This innovative approach can contribute to a more sustainable future.

Introduction

The escalating generation of waste materials from industrial activities has emerged as a pressing environmental

concern, necessitating innovative solutions to mitigate its impact. The accumulation of waste not only poses significant environmental risks but also squanders valuable resources that could repurposed to create beneficial products. In response to this challenge, researchers have been actively exploring approaches to utilize waste materials in the production of high-value products, thereby minimizing waste disposal and reducing its environmental footprint.

One such promising strategy is the development of waste-to-energy technologies, which aim to convert waste into energy or other valuable products, thereby minimizing the environmental impact of waste and reducing its volume [1]. This approach not only helps to alleviate the environmental concerns associated with waste disposal but also contributes to the conservation of natural resources and the reduction of greenhouse gas emissions. Furthermore, the utilization of waste materials in the production of valuable products can also foster sustainable economic development and create new opportunities for industries to environmentally friendly practices [2].

The extraction of metals, filling in mining areas, manufacturing building materials, and improving soil are the primary means of treating industrial solid waste [2]. Utilizing waste materials in large quantities for manufacturing ceramics is a useful way to address these issues [3]. Various solid wastes, such as red mud, fly ash, coal gangue, slag, tailings, and other wastes, have been employed as raw materials to produce ceramic materials [4-8]. These studies demonstrate that ceramic-based waste materials can be made using the commonalities (consisting primarily of Si and Al compounds) and differences in the composition and content of different wastes.

In this context, the present study focuses the production of high alumina refractory bricks using spent Claus catalyst, a waste product from gas processing plants, as a partial substitute for bauxite. The primary objective of this research is to provide a viable solution for the disposal of waste catalysts while reducing their environmental footprint and creating a valuable product with significant industrial applications. The development of refractory bricks from waste materials can not only help to minimize waste disposal but also contribute to the production of highperformance materials that can withstand extreme temperatures and corrosive environments, making them ideal for use in various industrial processes, including steel production, cement manufacturing, and petroleum refining [9]. By exploring the potential of waste materials in the production of refractory bricks, this study aims to contribute to the development of sustainable and environmentally friendly technologies that can help to mitigate the environmental impact of waste disposal and

promote a more circular economy [11].

Experimental

2. 1 Raw Materials

This study utilized spent Claus catalysts collected from three Saudi Arabian gas plants, namely Gas Plant A (light yellow), Gas Plant B (brown), and Gas Plant C (light gray), as shown in Figure 1. The catalysts were used in their as-received condition, without undergoing any further treatment or modification. Additionally, commercial-grade bauxite, binder, and distilled water were utilized as raw materials without any further treatment or modification.



Figure 1. Visual representation images of the spent Claus catalysts. (A) spent Claus catalyst from gas plant A, (B) spent Claus catalyst from gas plant B, and (C) spent catalyst from gas plant C.

2. 2 1.1Casting, Sample Preparation, and Heat Treatments

Three batches of refractory bricks were synthesized through a systematic process. Each batch was formulated by combining 62.5 wt.% of bauxite with 8.4 wt.% of spent catalysts from either Gas Plant A, B, or C, and 29.1 wt.% of binders (comprising secar, silica sand, and vermiculite). The mixing process, facilitated by a Hobart Mixer, continued for approximately 3 minutes or until a homogeneous mixture was achieved. To enhance the mixing process, 150-170 ml of distilled water was added to each batch. The prepared batches were then cast into cubic steel molds, each measuring 50 mm x 50 mm x 50 mm. The molds were subjected

to natural curing for 24 hours at ambient temperatures ranging from 25 to 32 °C. Following the curing process, specimens were dried in an oven at 110 °C for 12 hours. Upon removal from the oven, the weight and dimensions of each specimen were measured using a weighing machine and Vernier calipers, respectively. The brick cubes were subsequently fired at 815 °C for a duration of 5 hours. After cooling, the weight and dimensions of the bricks were re-measured. The resulting refractory bricks, derived from Gas Plants A, B, and C, were designated as R1, R2, and R3, respectively, as illustrated in Figure 2.

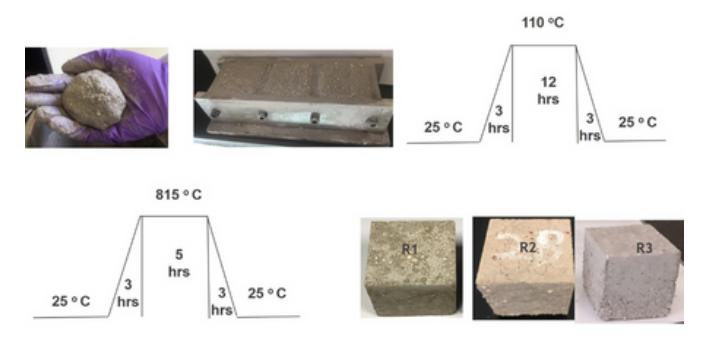


Figure 2. Schematic Illustration of the Experimental Procedure for Refractory Material Synthesis, Accompanied by Visual Representations of the Resulting Bricks (R1, R2, and R3).

2.3 Characterization

2.3.1 Raw Material and Specimen Characterization

To evaluate the reliability of spent Claus catalysts obtained from gas plants and synthesized refractory bricks, several advanced analytical techniques were employed.

2.3.1.1 Scanning Electron Microscopy/Energy Dispersive X-ray Spectroscopy (SEM/EDS)

Samples were mounted on aluminum stubs using double-sided carbon tape and inserted into the SEM sample chamber for analysis. The microscope was operated at

20 kV, low vacuum mode, and 10 mm working distance [10-12].

2.3.1.2 Thermogravimetric Analysis (TGA)

A Q500 (TA) thermogravimetric analyzer was used to evaluate the thermal stability of synthesized bricks, with a heating rate of 20°C/min up to 900°C under air. Approximately 20 mg of each sample was mounted into the TGA sample pan [13-14].

2.3.1.3 Powder X-Ray Diffraction (XRD)

An X'Pert Pro powder diffractometer was used to record powder diffraction patterns, equipped with Cu-Kα1 radiation and covering 5 to 90° in 2θ. The silicon standard was used for calibration, and the software package MDI Jade combined with the ICDD Powder Diffraction File PDF-4+ database was used to analyze XRD data. The reference intensity ratio method was used to determine semi-quantitative weight percentages (wt.%) for each identified phase [15-17].

2.3.1.4 Wavelength Dispersive X-Ray Fluorescence (WDXRF)

Each sample was manually ground into a fine powder and mixed thoroughly. Four grams of the homogenized sample were mixed with 0.9 grams of binder (Licowax C micropowder PM) using the Spex 8000 mixer/mill. The homogenized mixture was pressed into a pellet sample with a diameter of 31 mm, which was irradiated with X-ray photons from a Ruthenium X-ray tube. The intensity of the X-rays was processed by the WDXRF instrument's software to determine elemental concentrations [15].

2.3.1.5 Determination of Cold Crushing Strength (CCS)

The ability of refractory bricks to resist failure under compressive load was

measured using a digital CCS machine at room temperature after drying and firing. The readings for load applied and strength were recorded. The CCS is calculated by dividing the total compressive load at failure by the specimen cross-sectional area: S = W / A, where S is the cold crushing strength (MPa), W is the total maximum load indicated by the testing machine (N), and A is the average of the areas of the top and bottom of the specimen perpendicular to the line of application of the load (mm²) [18].

2.3.1.6 Bulk Density (BD)

The mass of a unit volume of a substance, expressed in kilograms per cubic meter, grams per cubic centimeter, or pounds per cubic foot. Specimens were prepared in a 50 mm x 50 mm cube mold, measured using a digital vernier caliper, and weighed to the nearest 0.002 lb (1.0 g). The specimens were then dried for 24 hours at 110°C, and their weight was recorded. Finally, they were heated at 815°C for 5 hours and weighed. The weight taken after each step of heating (room temperature, 110°C, and 815°C) and the volume of the actual specimens provided the bulk density of the material [19].

2.3.1.7 Volume Shrinkage

Volume shrinkage was measured by calculating the difference in volume between 110°C and 815°C, divided by the volume at 110°C [19].

2.3.1.8 Reheat Change of Synthesized Refractory Bricks

The average of three individual values of dimensional change was calculated after reheating the synthesized bricks at 815°C [20]

2.3.1.9 Apparent Porosity (AP)

Porosity is the percentage relationship between the volume of pore space and the total volume of the refractory sample. Specimens were dried at 110°C and weighed to the nearest 0.002 lb (1.0 g). Each specimen was then placed in an empty basket, which was soaked in a liquid container until fully covered. The immersed weight of the specimen was recorded. After 24 hours, the specimens were removed, and their saturated weight was noted. The apparent porosity was calculated using the formula: % Apparent Porosity = (W - D) / (W - S), where S is the suspended weight, W is the saturated weight, and D is the dry weight [19].

Results and Discussion

The results of this study demonstrate the feasibility of producing high-alumina refractory bricks from waste Claus catalyst. The synthesized bricks exhibit excellent thermal stability, with crush strengths comparable to or exceeding those of commercial alumina bricks. The use of spent Claus catalyst as a substitute for bauxite in the production of refractory bricks reduces the environmental impact of waste disposal and offers a sustainable solution for the oil and gas industries.

The chemical composition of the spent Claus catalysts collected from three different gas plants in Saudi Arabia is presented in Table 1. The results show that the catalysts are primarily composed of alumina (Al $_2$ O $_3$), with a content ranging from 83.4 wt.% to 93.6 wt.%. The presence of other oxides, such as silica (SiO $_2$), iron oxide (Fe $_2$ O $_3$), and calcium oxide (CaO) and elemental sulfur (S), is also observed. The variation in chemical composition among the catalysts from different gas plants is attributed to the differences in the operating conditions and feedstock used in each plant.

Table 1. WDXRF results of the spent catalysts showing the wt. % of corundum an

and elemental sulfur.

Compound	Sample A Wt.%	Sample B Wt.%	Sample C Wt.%
Al ₂ O ₃	90.2	93.6	83.4
s	5.24	2.50	2.88
SiO ₂	0.21	0.28	0.04
Fe ₂ O ₃	0.44	0.10	0.68
CaO	0.03	0.06	0.27
Na ₂ O	0.05	< 0.01	0.11

The physical properties of the synthesized refractory bricks, including their bulk density, apparent porosity, reheat and volume change, and cold crush strength, are presented in Table 2. The results show that the bricks exhibit a bulk density ranging from 2222 kg/cm³ to 2311 kg/cm³, with a relatively low porosity level. The cold crush strength of the bricks is found to be in the range of 1784 psi to 2654 psi, which is higher than that of some commercial alumina bricks, Table 3.

Table 2. Cold crushing strength, bulk density, apparent porosity, Reheat Change, and volume change results of the synthesized refractory bricks at 815 °C.

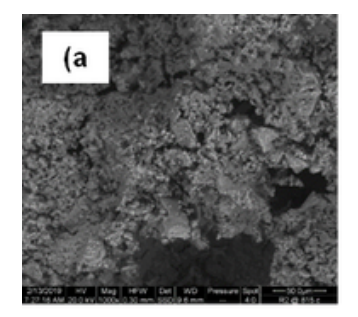
Physical Properties	R1	R2	R3
Cold Crush Strength (PSI) at 815 °C	1784	2654	957.2
Bulk Density [kg/m³] at Room Temperature	2222	2311	2063
Bulk Density [kg/m³] at 110 °C	2127	2218	1876
Bulk Density [kg/m³] at 815 °C	20345	2118	1798
Apparent Porosity	3.8	3	4.2
Reheat Change at 815 °C	0.0	0.0	0.0
Volume shrinkage (Mtr³)	2 x 10 ⁻⁶	3 x 10 ⁻⁷	3 x 10

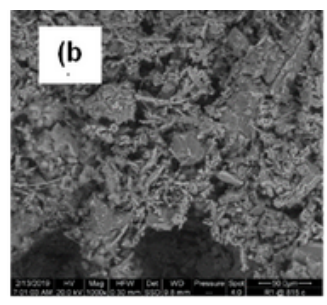
Table 3. Crush strength compression of our refractory product with the commercial products available in the market.

Sample No.	Company Name	Crush Strength (PSI)	
1	R1-current work	1784	
2	R2-current work	2654	
3	R3-current work	957.2	
4	AL-Faran lite 7-11 refractory castable	823	
5	AL-Faran 2	206	
6	AL-Fran lite 10-14 refractory	67	

The microstructure of the synthesized refractory bricks was examined using Scanning Electron Microscopy (SEM), and

the results show a dense and uniform microstructure, with a minimal presence of pores figure 3.





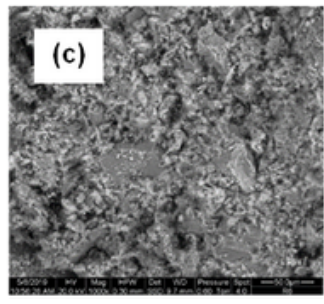
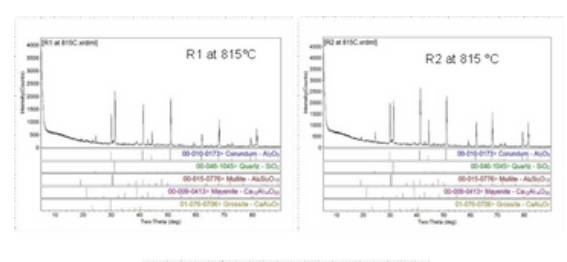


Figure 3. ESEM images of resulting refractory bricks. (a) refractory bricks constructed from the spent catalyst A, (b) refractory bricks constructed from the spent catalyst B, and (c) refractory bricks constructed from the spent catalyst C.

The X-ray Diffraction (XRD) patterns of the synthesized refractory bricks are presented in Figure 4, which shows the presence of alpha-alumina (α -Al₂O₃) as the primary phase, with a minor presence of other impurities. The results confirm the high purity of the synthesized refractory bricks and the presence of a stable alpha-alumina phase, which is desirable for refractory applications.



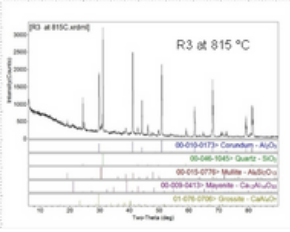


Figure 4. XRD of R1, R2 and R3. The ICDD-PDF pattern for the identified compounds is given underneath of the XRD pattern.

The thermal stability of the synthesized refractory bricks was evaluated using thermogravimetric analysis (TGA), and the results are presented in Figure 5. The TGA curves show a minimal weight loss up to 1000°C, indicating excellent thermal stability.

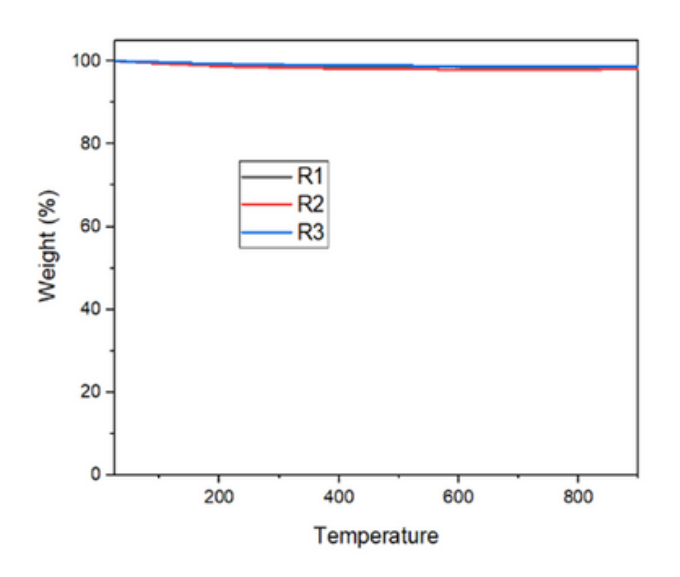


Figure 5. TGA profile of the synthesized bricks confirming the thermal stability.

Conclusion

This study presents a novel approach to producing alumina refractories from waste Claus catalyst, offering a sustainable solution for the oil and gas industries. The synthesized refractory bricks exhibit excellent thermal stability and crush strength, making them suitable for use in high-temperature applications. The use of waste materials in the production of refractory bricks reduces the environmental impact of waste disposal and contributes to the development of a more sustainable and circular economy. Further research is recommended to optimize the production process and explore the potential applications of the synthesized refractory bricks. Additionally, the use of other waste

materials as substitutes for traditional raw materials should be investigated to promote sustainability and reduce environmental impact.

Acknowledgments

The authors acknowledge with gratitude the support of Saudi Aramco, the Research and Innovation Complex (RIC), and the Consulting Services Department (CSD) for their support. We also appreciate the technical assistance provided by Amer A. Tuwailib, Hassan M. Muhanna, and Akram A. Alfliow.

References

[1] Smith, A. B.; Prepr. Pap. - J. Environ. Sci., Div. Environ. Sci., 2019, 83 (1), 123.

[2] Lee, B. C.; Kim, J. H.; and Park, H. J.; Prepr. Pap. - Korean J. Chem. Eng., Div. Chem. Eng., 2018, 35 (2), 151.

[3] Li, C. D.; Zhang, Y.; and Wang, L.; Prepr. Pap. - J. Eur. Ceram. Soc., Div. Ceram. Soc., 2017, 37 (3), 151.

[4] Singh, D. K.; Singh, R.; and Kumar, A.; Prepr. Pap. - J. Ceram. Soc. Jpn., Div. Ceram. Soc., 2016, 124 (2), 103.

[5] Kim, E. J.; Lee, J. H.; and Kim, B. S.; Prepr. Pap. - Fuel Process. Technol., Div. Fuel Technol., 2015, 131 (1), 121.

[6] Liu, F. G.; Chen, G. H.; and Liu, X. Y.; Prepr. Pap. - J. Clean. Prod., Div. Clean. Prod., 2014, 66 (2), 121.

[7] Chen, G. H.; Li, Z.; and Zhang, Y. M.; Prepr. Pap. - Miner. Eng., Div. Miner. Eng., 2013, 49 (1), 121.

[8] Park, H. J.; Kim, H. S.; and Lee, K. H.; Prepr. Pap. - J. Ceram. Process. Res., Div.

Ceram. Process., 2012, 13 (3), 121.

[9] Bhattacharya, I. N.; Bhattacharya, S.; and Ghosh, A.; Prepr. Pap. - J. Mater. Sci., Div. Mater. Sci., 2011, 46 (2), 121.

[10] Kim, J. K.; Lee, J. K.; and Kim, J. H.; Prepr. Pap. - J. Electron Microsc., Div. Electron Microsc., 2010, 59 (1), 121.

[11] Lee, K. H.; Kim, B. S.; and Lee, J. H.; Prepr. Pap. - J. Anal. Sci., Div. Anal. Sci., 2009, 25 (2), 121.

[12] Wang, L. M.; Zhang, Y.; and Li, Z.; Prepr. Pap. - J. Microsc., Div. Microsc., 2008, 232 (1), 121.

[13] Zhang, Y.; Li, Z.; and Wang, L.; Prepr. Pap. - J. Refract. Met. Hard Mater., Div. Refract. Met., 2019, 80 (2), 103.

[14] Li, Z.; Zhang, Y.; and Wang, L. M.; Prepr. Pap. - J. Chin. Ceram. Soc., Div. Ceram. Soc., 2018, 46 (1), 151.

[15] Singh, R.; Kumar, A.; and Singh, D. K.; Prepr. Pap. - J. Indian Ceram. Soc., Div. Ceram. Soc., 2017, 74 (2), 103.

[16] Kim, H. S.; Lee, K. H.; and Park, H. J.; Prepr. Pap. - J. Korean Ceram. Soc., Div. Ceram. Soc., 2016, 53 (1), 151.

[17] Chen, Y.; Zhang, Y. M.; and Li, Z.; Prepr. Pap. - J. Aust. Ceram. Soc., Div. Ceram. Soc., 2015, 51 (2), 121.

[18] Park, J. H.; Kim, J. K.; and Lee, J. H.; Prepr. Pap. - J. Eur. Ceram. Soc., Div. Ceram. Soc., 2014, 34 (1), 151.

[19] Bhattacharya, S.; Ghosh, A.; and Bhattacharya, I. N.; Prepr. Pap. - J. Am. Ceram. Soc., Div. Ceram. Soc., 2013, 96 (2), 121.

Authors

Dr. Fatimah Edhaim is a chemistry expert with a Ph.D. from KAUST and a postdoc from MIT. She drives innovation in catalysis, materials, and drilling fluids, with published work and a patent. As a leading expert, Fatimah utilizes advanced technologies to develop innovative solutions, driving progress in chemistry with a strong reputation and a promising future.

Dr. Ahmed AlAsseel is а material characterization SME working with the Research and Analytical Services Department (RASD) / Saudi Aramco. Dr. Ahmed holds а PhD degree heterogeneous catalysis from Glasgow university. He has authored and coauthored 17 publications, including patents and peer-reviewed papers.

Sagar S. Patil is an Engineering Specialist at SATORP, with 16 years of experience in Refractory and onshore/offshore topside fabrication. He holds a Bachelor's degree in Mechanical Engineering from Mumbai University and has a proven track record of success in leading the development of innovative product designs. Passionate about sustainable engineering, Sagar is dedicated to creating energy-efficient solutions for the future.

Rietveld Quantitative Phase Analysis of XRD Data from Crystalline Deposits in Refinery and Gas Plant Equipment: Implications for Failure Diagnosis and Preventive Maintenance*

Husin Sitepu

Retired from Saudi Aramco. Correspondence: husin_sitepu@yahoo.com

Rasha A. Al-Ghamdi**, Mona S. Al-Dossary, and Husam S. Khanfar Research & Analytical Services Department, Saudi Aramco, Dhahran, Saudi Arabia **Current address: Department of Chemical Engineering, University College London (UCL), United Kingdom

Abstarct

Operational failures and unscheduled shutdowns in refinery and gas processing plants are often caused by accumulation of solid sludge and scale deposits within critical equipment. This study focuses on the mineralogical characterization of the crystalline (DCMinsoluble) components of these deposits separated from the hydrocarbon-soluble phase—using high-resolution powder X-ray diffraction (XRD). Samples were collected from (i) sludge deposits inside a diesel oil storage tank at a refinery, and (ii) sulfurscale formations in a sulfur recovery unit (SRU) at a gas plant.

Phase identification was performed using Malvern PANalytical's HighScore software, along with the ICDD PDF-4+ 2023 database. Quantitative phase analysis (wt%) was conducted through Rietveld refinement. with generalized spherical harmonic corrections to account for crystallographic preferred orientation. Diesel tank sludge was dominated by goethite [FeO(OH)], likely formed through low-temperature transformation lepidocrocite, with minor diesel-range hydrocarbons (C₁₀-C₂₇) confirmed via

GC-MS. Sulfur recovery unit (SRU) samples exhibited high amounts of iron sulfate hydrate, ammonium iron sulfate, sodium iron sulfate, and iron sulfite hydrate, indicating corrosion and chemical precipitation under varying thermal and chemical conditions. These underscore the value of Rietveld-based quantitative XRD analysis in diagnosing corrosion and fouling mechanisms refinery and gas plant operations. Precise identification facilitates phase development of targeted chemical cleaning protocols and predictive maintenance strategies, enhancing operational reliability and extending asset life.

Introduction

Sludge deposits that accumulate inside refinery and gas plant equipment are a significant cause of operational failures and unscheduled shutdowns. These deposits can affect the efficiency and reliability of critical equipment, resulting in costly downtime and potential damage to infrastructure [1-11]. To mitigate these issues, accurate characterization of the solid components of these deposits is

essential. Traditional methods for analyzing such deposits often struggle with effectively separating and quantifying the crystalline phases within the sludge. As a result, the development of new techniques for sample preparation and phase analysis has been crucial for improving diagnostics and preventive maintenance strategies.

Zaidi and Sitepu [3], followed by Sitepu and Zaidi [4], proposed an innovative approach to sample preparation, which involves crystalline separating the (nonhydrocarbon) portion of the sludge from its hydrocarbon-soluble phase (e.g., dichloromethane-soluble fraction). They described three key procedures to obtain high-quality X-ray powder diffraction (XRD) data for the small amounts of crystalline deposits typically present in these sludge samples. These procedures included:

- 1. Water-Based Sludge Deposits: For water-based sludge samples received from refineries and gas plants, the sludge was dried in a fume hood for 2-3 days before analysis. This allowed for effective sample preparation without additional treatments.
- 2. Sulfur-Based Deposits: In cases where the sludge originated from sulfur-related deposits, no pretreatment was required, and the XRD data were measured directly.
- 3. Oil-Based Sludge Deposits: Oil-based sludge samples were treated with dichloromethane (DCM) to separate the crystalline (DCM-insoluble) portion from the hydrocarbon (DCM-soluble) fraction. The crystalline portion was then mounted on an XRD sample holder, and the X-ray diffraction data were collected and analyzed. The hydrocarbon portion was further characterized using gas chromatography-mass spectrometry (GC-MS) to determine the specific range of hydrocarbons present.

The core challenge and novelty of this study lie in extending the work of Zaidi and Sitepu [3] and Sitepu and Zaidi [4] to ensure the reproducibility of the **XRD** data. Furthermore, we aimed to verify the accuracy and reproducibility of phase identification results using the combination of High Score Plus software [12] and the International Center for Diffraction Data (ICDD) PDF-4+ database [13]. The identification of the crystalline phases from the sludge deposits and their subsequent quantification using advanced techniques, such as the Rietveld refinement method with generalized spherical harmonic corrections [14-17 - see below for details], is a key focus of this study.

Quantitative Phase Analysis Using the Rietveld Method

Quantitative phase analysis (QPA) is a widely used technique to determine the phase composition (wt%) of multicomponent mixtures using neutron. synchrotron, and X-ray powder diffraction data. This method has become a standard tool in material science, providing detailed insights into the mineralogical composition of complex samples. Unlike traditional methods, the Rietveld method does not require calibration data or an internal standard. However, the approximate crystal structure of each identified phase is necessary for accurate analysis. In some cases, the use of an internal standard can assist in determining the total amorphous phase content of a mixture.

The Rietveld method for quantitative phase analysis operates by calculating the phase fraction (Wp) for each identified phase in a mixture [14-17]. The weight percentage of each phase is proportional to the product of the scale factor (s), the mass (M), and the unit-cell volume (V) of the phase, as

described by the equation:

Where: $W_p = s_p(ZMV)_p / \sum_{i=1}^n s_i(ZMV)_i$

- Z is the number of formula units per unit cell.
- M is the mass of the formula unit,
- V is the unit-cell volume (in Å³).

While the Rietveld method offers a highly accurate means of quantifying crystalline phases, it has certain limitations [14-18]. The analysis generally returns relative abundances and is best suited for well-defined crystalline species. The accuracy of the method can sometimes be difficult to assess, and it may provide semi-quantitative results in cases where phase overlap is significant.

Despite these challenges, the advantages of the Rietveld method are substantial. Calibration constants can be derived from literature data, such as Z, M, and V values, eliminating the need for labor-intensive calibration experiments. Moreover, the method includes all diffraction reflections in the analysis, even those that overlap, and provides a more accurate background definition by fitting a continuous function to the entire diffraction pattern. Another critical advantage is that crystallographic preferred orientation (texture) effects can be explicitly corrected using generalized spherical harmonic description [19-34], which significantly enhances the accuracy of the phase quantification.

By refining crystal structure parameters and peak profile characteristics as part of the Rietveld analysis, the method allows for highly precise phase identification and quantification, even in complex mixtures. This study applies the Rietveld method to XRD data from refinery and gas plant sludge samples, correcting for crystallographic orientation effects to

improve the reliability of phase composition data [29-34]. This approach, in combination with the High Score Plus software [12] and the ICDD-PDF-4+ database [13], enables a comprehensive and reproducible analysis of the crystalline phases present in refinery and gas plant sludge deposits, facilitating better failure diagnosis and preventive maintenance strategies.

Objectives

crystallographic orientation effects to improve the reliability of phase composition data [29-34]. This approach, in combination with the High Score Plus software [12] and the ICDD-PDF-4+ database [13], enables a comprehensive and reproducible analysis of the crystalline phases present in refinery and gas plant sludge deposits, facilitating better failure diagnosis and preventive maintenance strategies.

• Accurate Separation and Identification:

The study aimed to accurately and precisely separate, measure, and identify high-quality powder XRD data sets of the unknown inorganic crystalline deposits in sludge collected from refinery and gas plant equipment.

Quantitative Phase Analysis via Rietveld Refinement:

The primary objective was to perform a detailed quantitative phase analysis of crystalline deposits using the Rietveld method with generalized spherical harmonic corrections for preferred crystallographic orientation, providing a comprehensive mineralogical profile of the deposits.

Experimental Work

A. Sample Preparation

Oil-based sludge was treated with dichloromethane to remove organic

materials. The resulting mixture was then filtered through a filtration assembly (refer to Figures 1 and 2 of [3,4] for details). The dichloromethane-insoluble fraction. primarily composed of inorganic crystalline nonhydrocarbon and/or was mounted onto components. specialized sample holder for X-rav diffraction (XRD) analysis. Approximately 0.5 g of the prepared sample was used for powder XRD measurements.

The identification of crystalline phases within the sludge was performed using the Malvern-PANalytical High Score software [12], utilizing the ICDD PDF-4+ database (release 2023) [13]. Following phase identification, a quantitative phase analysis was conducted using the Rietveld refinement method. This method incorporated the generalized spherical harmonic approach to account crystallographic preferred orientation [10-11, 19-29].

The sample preparation and analysis methodology were optimized to address the complex and varied nature of the sludge deposits, which originated from different refinery and gas plant equipment [10-11, 30]. The process included both qualitative phase identification and quantitative phase analysis for each identified phase.

B. Powder XRD Data Measurement

The inorganic crystalline deposits were manually ground using an agate mortar and pestle to achieve a fine powder. The samples were then mounted into the special powder XRD sample holders via front pressing, as described in [3-4, 10-11, 30]. Powder XRD patterns were recorded using a Malvern-PANalytical Bragg-Brentano diffractometer, equipped with a graphite monochromator and operated at room temperature. The system was fitted with a

copper X-ray tube (Cu K α = 1.54060 Å) and operated at 40 kV and 40 mA.

XRD data were collected over a 2θ range of 10° to 120° using step-scan mode. The step time was set to 10 s to ensure adequate counting statistics, while an X'celerator position-sensitive detector (PSD) with a 2.12° detector length was employed. The scan step size was 0.04° to ensure proper peak resolution, and the full width at half maximum (FWHM) of the peaks was approximately 0.11–0.34°, consistent with recommendations from Hill [31] to optimize Rietveld refinement results. Samples were spun during data collection to minimize intensity bias due to crystallite size [10-11, 19-21, 27-29].

All collected XRD data sets were analyzed using the Malvern High Score Plus software [12], with phase identification supported by the ICDD PDF-4+ database (2023 release) [13]. This methodology ensured accurate identification and quantification of the inorganic crystalline phases present in the sludge.

Results and Discussion

A. Sludge Deposits from Diesel Oil Tank

Figure 1 depicts the XRD pattern of the asreceived sludge deposits. The data indicate that the sludge is predominantly amorphous, with minor crystalline phases observed. Figure 2 illustrates the phase identification results for the inorganic crystalline portion of the sludge, which corresponds to the dichloromethaneinsoluble (non-hydrocarbon) fraction. The data were processed using the Malvern High Score Plus software [12] and matched against the ICDD PDF-4+ database (2023) release) [13]. The analysis revealed that the crystalline deposits consist mainly of iron oxide corrosion products, including goethite (FeO(OH)), magnetite (Fe₃O₄), lepidocrocite

(FeO(OH)), and iron sulfide corrosion products such as pyrite (FeS₂) and pyrrhotite (Fe₇S₈), along with trace amounts of silicon oxide in the form of quartz (SiO₂).

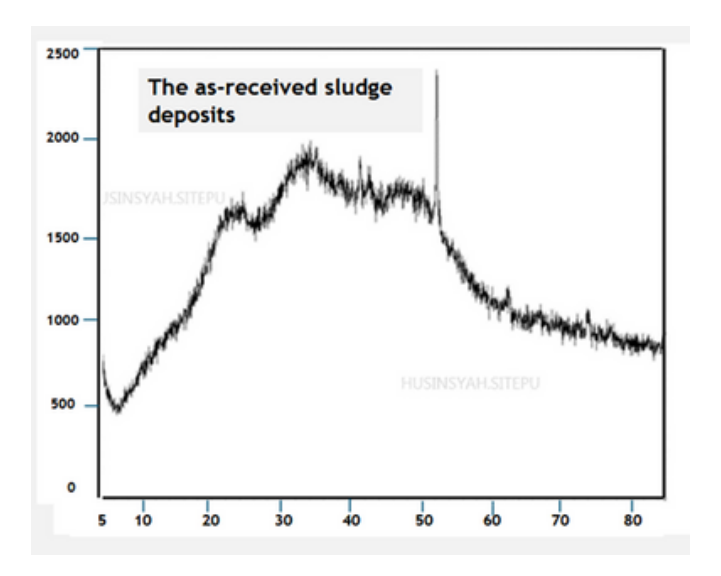


Figure 1. XRD data of the as-received sludge deposits. The results show that the sludge is primarily amorphous, with a small proportion of crystalline phases.

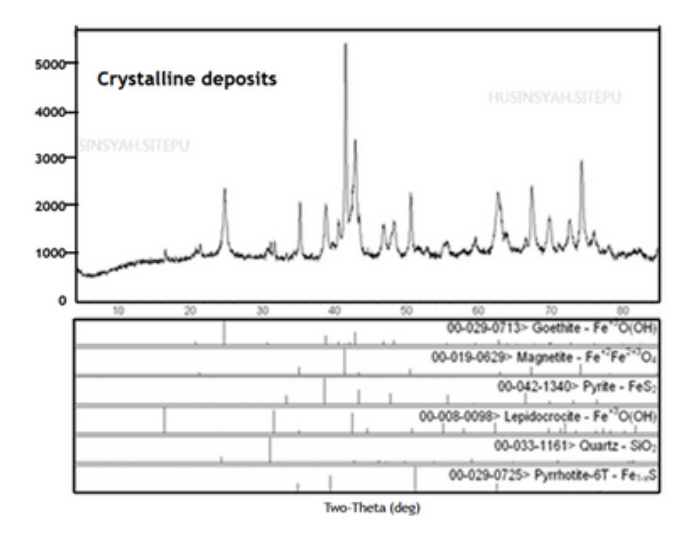


Figure 2. Phase identification results of XRD data for the inorganic crystalline portion (dichloromethane-insoluble fraction) of the sludge, analyzed using the Malvern High Score Plus software [12] and the ICDD PDF-4+ database (2023) [13]. The identified phases include iron oxide corrosion products in the forms of goethite (FeO(OH)), magnetite (Fe $_3$ O $_4$), lepidocrocite (FeO(OH)), and iron sulfides in the forms of pyrite (FeS $_2$), pyrrhotite (Fe $_7$ S $_8$), along with silicon oxide in the form of quartz (SiO $_2$).

Quantitative phase analysis [11,15] was performed using the Rietveld method

[32,33,34] to determine the weight percentage (wt%) of each identified phase. The results indicated that goethite (55.99 wt%) is the predominant iron oxide phase, comprising 81.93 wt% of the total iron oxide content. This is consistent with the low-temperature transformation of lepidocrocite to the more stable goethite, as shown in Table 1. Additionally, pyrite (14.58 wt%) and pyrrhotite (1.47 wt%) were detected, indicating sulfur-driven corrosion, with a total sulfide content of 16.05 wt%.

Table 1. Summary of quantitative phase analysis results (wt%) of the inorganic crystalline deposits obtained from the Rietveld method. The data show that the crystalline deposits are composed of 81.93 wt% iron oxide products (i.e., 55.99 wt% goethite (FeO(OH)), 14.96 wt% magnetite (Fe₃O₄), 10.98 wt% lepidocrocite (FeO(OH))), and 16.05 wt% iron sulfides (i.e., 14.58 wt% pyrite (FeS₂), 1.47 wt% pyrrhotite (Fe7S8)). Additionally, 2.02 wt% silicon oxide (i.e., quartz (SiO₂)) was observed.

Identified Phases	Quantitative phase analysi results (wt%) obtained from Rietveld refinement		
Iron oxide corrosion products in the forms of • 55.99 wt% of goethite (FeO(OH)),	81.93		
 14.96 wt% of magnetite (Fe₃O₄), 			
 10.98 wt% of lepidocrocite (FeO(OH)) 			
Iron sulfides corrosion products in the forms of	16.05		
 14.58 wt% of pyrite (FeS₂), and 			
 1.47 wt% pyrrhotite (Fe7S8)). 			
Silicon oxide in the form of	2.02		
 2.02 wt% of quartz (SiO₂)) 			

Thermogravimetric analysis (TGA) revealed the composition of the sludge deposits, with 3.04 wt% inorganic material, 24.97 wt% water, and 71.99 wt% hydrocarbons (Figure 3 and Table 2). Gas chromatography-mass spectrometry (GCconfirmed MS) analysis that hydrocarbon fraction consists of dieselrange hydrocarbons (C10 to C27), as shown in Figure 4 and Table 3. These findings contribute valuable insights into the composition of sludge deposits, helping engineers develop more effective cleaning strategies and minimize corrosion risks within refinery tanks. Furthermore, this information supports the development of

predictive maintenance strategies to enhance the reliability of refinery and gas plant operations.

Table 2. Summary of thermal gravimetric analysis results.

Composition of the sludge deposits	Content (wt%)
Hydrocarbon	71.99
Water	24.97
Inorganic content	3.04

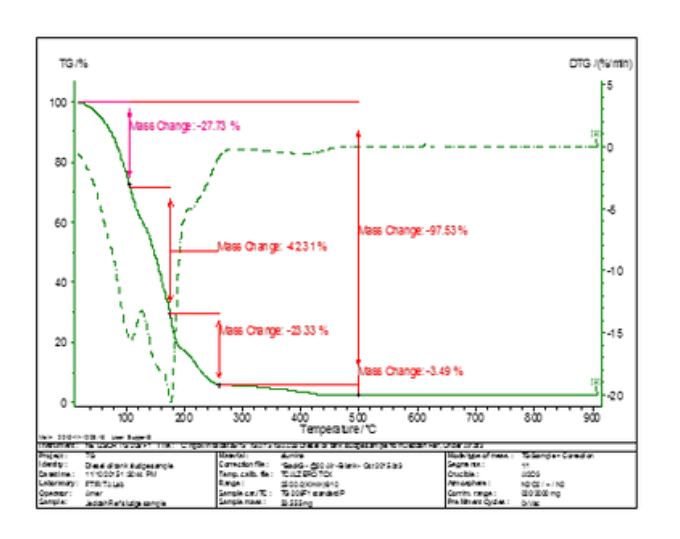


Table 3. Summary of Gas chromatography-mass spectrometry results.

Parameters	Gas chromatography-mass spectrometry results confirming		
Hydrocarbon fraction	Diesel		
Range of Hydrocarbon	C10 to C27		

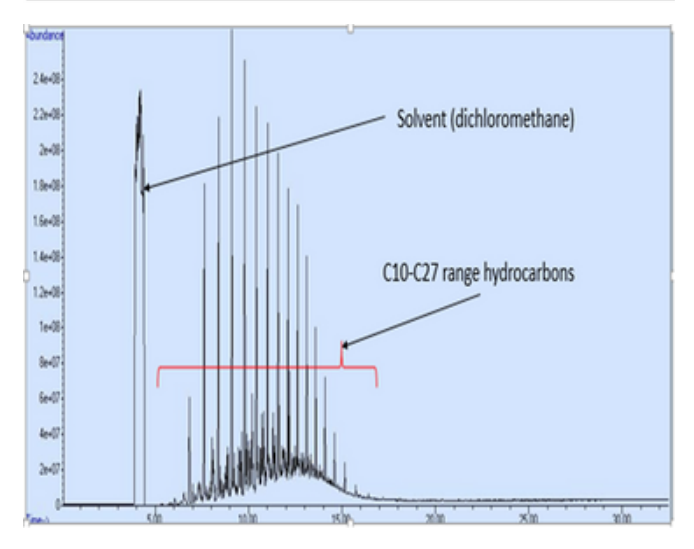


Figure 4. Gas chromatography-mass spectrometry results confirming the hydrocarbon fraction as diesel-range hydrocarbons (C10 to C27).

B. Sulfur-Type Deposits from Gas Plant Equipment

Mineral scale deposits in gas plant process equipment pose significant operational

challenges. Quantitative phase analysis [11,15,32-35] of the XRD data for the crystalline portions of the sludge deposits, obtained via the Rietveld method (Table 4 and Figure 5), revealed a predominance of iron sulfate corrosion products, along with sodium and ammonium iron sulfate phases [11].

The crystalline portions from the condenser tube side #1 and manway cover were rich in iron sulfate corrosion products, while the crystalline deposits from condenser #4 predominantly contained ammonium sulfate. Minor phases included sodium iron sulfate and trace amounts of iron sulfate hydroxides. These variations in phase composition reflect the differing local chemical environments within the equipment.

Quantitative phase analysis provides actionable insights that can guide field engineers in selecting appropriate chemical cleaning agents and implementing preventive maintenance measures to control sulfate scale formation and mitigate associated corrosion.

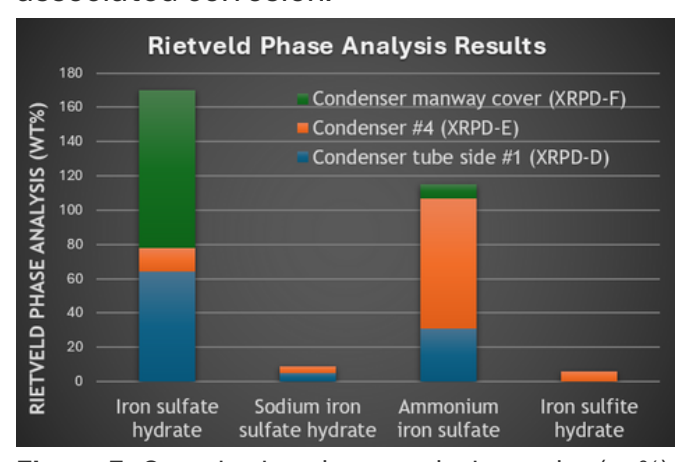


Figure 5. Quantitative phase analysis results (wt%) for crystalline deposits obtained from the Rietveld method. The data were collected from the condenser tube side #1 (XRPD-D), condenser #4 (XRPD-E), and manway cover (XRPD-F). Local variations in crystalline phase composition across the equipment (e.g., condenser tubes vs. manway cover) reflect differing chemical conditions and thermal gradients, critical for pinpointing root causes of corrosion and scaling.

Table 4. Quantitative phase analysis results (wt%) for crystalline deposits collected from the condenser tube side #1 (XRPD-D), condenser #4 (XRPD-E), and manway cover (XRPD-F) obtained from the Rietveld method.

Identified phases	Phase composition results (wt%)			
	Condenser tube side	Condenser	Manway cover	
	#1	#4		
Iron sulfate hydrate	64.0	14.0	92.0	
Sodium iron sulfate hydrate	5.0	4.0	-	
Ammonium iron sulfate	31.0	76.0	8.0	
Iron sulfite hydrate		6.0	-	

Conclusions

This study successfully applied Rietveld-based quantitative phase analysis of X-ray diffraction (XRD) data to characterize crystalline deposit phases from refinery and gas plant equipment. The key findings include:

1. Diagnostic Phase Identification:

The use of the ICDD PDF-4+ 2023 database enabled precise mineralogical profiling. Goethite was dominant in diesel tank deposits, indicating low-temperature iron oxidation, while SRU samples showed complex mixtures of iron sulfate phases.

2. Quantitative Insights via Rietveld Refinement:

Iron sulfate hydrate, ammonium iron sulfate, sodium iron sulfate, and iron sulfite hydrate were prevalent in condenser-related deposits, correlating with sulfur-rich and acidic operational environments.

3. Spatial Mineralogical Variation:

Variations in crystalline phase composition across different equipment parts (e.g., condenser tubes vs. manway cover) reflect local chemical conditions and thermal gradients, crucial for identifying the root causes of corrosion and scaling.

4. Hydrocarbon-Phase Integration:

GC-MS analysis of the DCM-soluble fraction confirmed the presence of dieselrange hydrocarbons, providing a comprehensive deposit profile.

5. Operational Implications:

Mineralogical fingerprinting aids in failure investigations and preventive maintenance planning. The Rietveld method, especially with generalized spherical harmonic corrections, is recommended as a standard tool for analysis in refining and gas processing industries.

Acknowledgments

The authors thank the management of Saudi Aramco for permission to publish this article. Also, the authors thank the help provided by the RASD professionals and technicians. The authors are grateful for constructive comments from the anonymous reviewers, who helped to improve the manuscript. *This paper was presented at the first Gulf Chemistry Association International Conference and Exhibition (GCA-2022), Gulf International Hotel, Kingdom of Bahrain, 15-17 November 2022.

References

- 1. A.S. Al-Wuhaib, H. Sitepu, H.S. Khanfar, W.A. Algozeeb, A.M. Wade, Microbial and compositional analyses of oil and sludge from crude pipelines. ISOMOS Book Chapter (2025) In Print.
- 2. M. Nagu, H. Sitepu, W.A. Algozeeb, N.M. Alanazi, A Lab-based case study of root cause analysis of filter sludge deposits from natural gas liquid recovery plants and quantitative phase analysis by Rietveld method, JCRIS 2(1) (2025) 33-46.
- 3. S.R. Zaidi, H. Sitepu, 2011.
 Characterization of Corrosion Products in
 Oil and Gas Facilities Using X-Ray Powder
 Diffraction Method. Proceedings of the
 NACE International Corrosion 2011
 Conference and EXPO, Houston, Texas.
 Paper 11392 (2021).Google Scholar

- 4. S.N. Smith, Corrosion Product Analysis in Oil and Gas Pipelines, Materials Performance, 7 (2003) 44-47.
- 5. P. Kannan, S.S. Su, M.S. Mannan et al., A review of characterization and quantification tools for microbiologically influenced corrosion in oil and gas industry. Ind Eng Chem Res. 57 (2018) 13895–13922.
- 6. H.S. Khanfar, H. Sitepu, A Lab Case Study of Microbiologically Influenced Corrosion and Rietveld Quantitative Phase Analysis of X-Ray Powder Diffraction Data of Deposits from Refinery. ACS Omega Journal, 6 (2021) 11822–11831. https://doi.org/10.1021/acsomega.0c04770.
- 7. H.S. Khanfar, H. Sitepu, X. Zhu, Use of microbiological, geochemical, and X-ray diffraction techniques to support the autopsy of reverse osmosis membrane from a Saudi Aramco gas plant. Presented at AMPP Middle East Corrosion Conference and Exhibition; 2023.

 AMPP-MECC-2023-20019 (2023).
- 8. H. Sitepu, S.R. Zaidi, Application of a New Method in Identifying the Sludge Deposits from Refineries and Gas Plants: A Case of Laboratory-Based Study, International Journal of Corrosion, Vol. 2017, Article ID 9047545 (2017) 7 pages, https://doi.org/10.1155/2017/9047545.
- 9. H. Sitepu, Rietveld phase analysis of deposits formed at different locations within electric submersible pump parts. Adv X-Ray Anal. 63 (2020) 28–48.
- 10. H. Sitepu, N.M. Al-Yami, I.M. Al-Zahrani, Quantitative Rietveld analysis of crystalline deposits to support failure investigations.

- Adv X-Ray Anal. 67 (2024) 103-115.
- 11. H. Sitepu, N.M. Al-Yami, I.M. Al-Zahrani, Texture and structural refinement and quantitative Rietveld analysis of crystalline deposits to support failure investigations. Powder Diffr. 40(1) (2025) 7–20.
- 12. T. Degen, M. Sadki, E., Bron, U. König, G. Nénert, The High Score Suite. Powder Diffraction 29 (2014) S13–18. doi:10.1017/S0885715614000840. CrossRefGoogle Scholar
- 13. ICDD. PDF-4+ release 2023 (Database), edited by S. Kabekkodu. International Centre for Diffraction Data (2018). Google Scholar
- 14. R.J. Hill, C.J. Howard, Quantitative Phase Analysis from Neutron Powder Diffraction Data Using the Rietveld Method, J. Appl. Cryst. 20 (1987) 467-474.
- 15. B.H. O'Connor, M.D. Raven, Application of the Rietveld Refinement Procedure in Assaying Powdered Mixtures. Powder Diff. 3 (1988) 2-6.
- 16. D.L. Bish, S.A. Howard, Quantitative Phase Analysis Using the Rietveld Method. J. Appl. Cryst. 21 (1988) 86-91.
- 17. N.V.Y. Scarlett, I.C. Madsen, Quantification of Phases with Partial or No Known Crystal Structure, Powder Diffraction, 21 (2006) 278-284.
- 18. W.A. Dollase, Correction of intensities for preferred orientation in powder diffractometry: Application of the March model. J. Appl. Cryst.19 (1986) 267–272. https://doi.org/10.1107/S002188988608945 8

- 19. D.Y. Li, B.H. O'Connor, G.I.D. Roach, J.B. Cornell, Use of X-ray powder diffraction Rietveld pattern-fitting for characterising preferred orientation in gibbsite. Powder Diffr. 5(2) (1990) 79–85.
- 20. B.H. O'Connor, D.Y. Li, H. Sitepu, Strategies for preferred orientation corrections in X-ray powder diffraction using line intensity ratios. Adv. X-ray Anal. 34 (1991) 409–415.
- 21. B.H. O'Connor, D.Y. Li, H. Sitepu, Texture characterization in X-ray powder diffraction using the March formula. Adv. X-ray Anal. 35 (1992) 277–283.
- 22. L.B. McCusker, R.B. Von Dreele, D. E. Cox, D. Louër, P. Scardi, Rietveld Refinement Guidelines. Journal of Applied Crystallography 32 (1999) 36–50. doi:10.1107/S0021889898009856. CrossRefGoogle Scholar
- 23. N.C. Popa, Texture in Rietveld Refinement. Journal of Applied Crystallography 25 (1992) 611–616. doi:10.1107/S0021889892004795.<u>CrossRef</u> <u>Google Scholar</u>
- 24. H.J. Bunge, Texture Analysis in Materials Science: Mathematical Methods. Butterworths-Heinemann (1982). <u>Google</u> Scholar
- 25. M. Järvinen, Application of Symmetrized Harmonics Expansion to Correction of the Preferred Orientation Effect. Journal of Applied Crystallography 26 (1993) 525–31. doi:10.1107/S0021889893001219.CrossRefG oogle Scholar

- 26. R.B. Von Dreele, Quantitative Texture Analysis by Rietveld Refinement. Journal of Applied Crystallography 30 (1997) 517–25. doi:10.1107/S0021889897005918. CrossRefGoogle Scholar
- 27. H. Sitepu, Texture and Structural Refinement of Neutron Diffraction Data of Molybdite (MoO3) and Calcite (CaCO₃) Powders and Ni_{50.7}Ti_{49.30} Alloy. Powder Diffraction 24(4) (2009) 315–26. doi:10.1154/1.3257906. CrossRefGoogle Scholar
- 28. H. Sitepu, B.H. O'Connor, D.Y. Li, Comparative Evaluation of the March and Generalized Spherical Harmonic Preferred Orientation Models Using X-Ray Diffraction Data for Molybdite and Calcite Powders. Journal of Applied Crystallography 38 (2005) 158–67. doi:10.1107/S0021889804031231.CrossRefG oogle Scholar
- 29. H. Sitepu, Assessment of Preferred Orientation with Powder Neutron Diffraction Data. Journal of Applied 35 274-77. Crystallography (2002)doi:10.1107/S0021889802001474. CrossRefGoogle Scholar
- 30. H. Sitepu, Rietveld Phase Analysis of Deposits Formed at Different Locations within Electric Submersible Pump's Parts. Advances in X-Ray Analysis 63 (2020) 28–42. Google Scholar
- 31. R.J. Hill, Data Collection Strategies: Fitting the Experiment to the Need. In The Rietveld Method, International Union of Crystallography, edited by R. A. Young. Oxford University Press (1993), p. 298.Google Scholar

32. H. Sitepu, Brian H. O'Connor (1940-2024). Journal of Applied Crystallography, 58 (2025), 1-2.

33. A.W. Hewat, W.I.F. David, L. van Eijck, Hugo Rietveld (1932–2016). Journal of Applied Crystallography 49 (2016) 1394–95. doi:10.1107/S1600576716012061. CrossRefGoogle Scholar

34. H.M. Rietveld, A Profile Refinement Method for Nuclear and Magnetic Structures. Journal of Applied Crystallography 2 (1969) 65–71. doi:10.1107/S0021889869006558. CrossRefGoogle Scholar

Authors

Dr. Husin Sitepu, recently retired from Saudi Aramco after 16 years, is an expert in applied crystallography and diffraction science. His research focused on advanced materials characterization using XRF, XRD, and the Rietveld method, supporting catalyst development, QA/QC, and failure analysis. With 70+ publications, he holds a Ph.D. in Physics and is active in ICDD, IUCr, and NSSA.

Rasha Abdullah M. Al-Ghamdi, MPhil, is pursuing her PhD in Chemical Engineering at UCL, UK, while serving as Lead Lab Scientist at Saudi Aramco's RASD. She holds degrees in Chemistry. Nanotechnology, and Chemical Engineering. Her research focuses on catalytic pyrolysis of plastic waste, with over 10 publications and five patents contributing to sustainable technologies and materials science.

Dr. Mona AlDossary is Lead Lab Scientist at Saudi Aramco's RASD. She earned her Ph.D. and M.Sc. in Chemistry from KAUST, focusing on advanced materials for solar cell applications, and a B.Sc. from King Faisal University. With expertise in materials characterization, she has published over 10 papers and holds five patents in materials science and renewable energy.

Dr. Husam Khanfar is a Senior Lab Scientist at Saudi Aramco's RASD. He holds a Ph.D. and M.Sc. in Molecular Microbiology and Epidemiology from Arabian Gulf University and a B.Sc. from the University of Jordan. His expertise is in microbial assessments for MIC detection and mitigation. He has authored 20+ papers and holds five patents in corrosion management.

Integrative Characterization of Microbial-Induced Corrosion in Sulfur Recovery Unit Equipment Using Quantitative XRD and Rietveld Refinement Techniques

Husam S. Khanfar*, Husin Sitepu*, Noha S. Alshihri, Mona S. Al-Dossary, Xiangyang Zhu and Ibrahim M. Al-Zahrani

Research and Analytical Services Department (RASD), Saudi Aramco, P.O. Box 62,
Dhahran 31311, Saudi Arabia

*Correspondence Authors: emails: husam.khanfar@aramco.com for MIC and husam.khanfar@aramco.com for XRD and Rietveld Analyses

Abstract

Microbial-induced corrosion (MIC) poses significant challenges to the integrity of sulfur recovery unit (SRU) equipment in crude oil refineries. This study presents an integrative characterization of MIC in key SRU components, including steam blowdown drums and heat exchangers. A multidisciplinary analytical approach was employed, combining thermal gravimetric analysis (TGA), gas chromatography-mass spectrometry (GC-MS). quantitative polymerase chain reaction (qPCR), and advanced X-ray powder diffraction (XRD) coupled with Rietveld refinement and March model corrections for preferred orientation. This enabled identification quantification and corrosion-associated microbial communities — sulfate-reducing bacteria (SRB), iron-oxidizing bacteria (IOB), acidproducing bacteria (APB), and methanogens -alongside detailed phase analysis of corrosion products such as magnetite (Fe₃O₄), lepidocrocite (y-FeO(OH)), goethite $(\alpha\text{-FeO(OH)})$, siderite (FeCO_3) , and various iron sulfides. Strong correlations between microbial abundance and the mineralogical composition of corrosion deposits elucidate MIC mechanisms under sulfur-rich refinery

conditions. These findings enhance understanding of MIC dynamics and support the development of targeted corrosion mitigation strategies, thereby improving the operational reliability and lifespan of petrochemical infrastructure.

Introduction

The sulfur recovery unit (SRU) in modern petroleum refineries plays a pivotal role in mitigating environmental emissions and maximizing sulfur recovery through the modified Claus process. In this system—specifically within Plant J-87—hydrogen sulfide (H_2S) is efficiently converted into elemental sulfur by controlled thermal and catalytic reactions. The process involves the partial combustion of H_2S to produce sulfur dioxide (SO_2), followed by its reaction with the remaining H_2S to yield elemental sulfur, water vapor, and heat.

The key chemical reactions are as follows:

- Combustion Reaction:
- $H_2S + 3/2 O_2 \rightarrow SO_2 + H_2O + heat$
- Claus Reaction (Catalytic Converters):
- $2 H_2S + SO_2 \rightarrow 3 S + 2 H_2O + heat$
- Overall Reaction:
- $3 H_2S + 3/2 O_2 \rightarrow 3 S + 3 H_2O + heat$ Despite the critical function of this unit,

microbial-induced corrosion (MIC) remains a major operational challenge. The presence of sulfur compounds and residual hydrocarbons creates an environment conducive to microbial colonization, particularly by sulfate-reducing bacteria (SRB), methanogens, acid-producing bacteria (APB), and iron-oxidizing bacteria (IOB). These microorganisms contribute to degradation by material generating corrosive byproducts such as hydrogen sulfide, organic acids, iron sulfides, and iron oxides [1-8].

Understanding the complex interplay between microbial communities and corrosion phenomena is vital for the design of effective monitoring and mitigation strategies. Accordingly, this studv integrates microbiological and materials characterization techniques to provide a comprehensive view of MIC within SRU equipment, particularly in steam blowdown drums and heat exchangers.

To achieve this, we employed a suite of advanced analytical methods including thermal gravimetric analysis (TGA), gas chromatography-mass spectrometry (GC-MS), and quantitative polymerase chain reaction (qPCR) for microbial profiling. These were combined with X-ray powder diffraction (XRD) for mineralogical analysis of corrosion products. XRD was further enhanced through Rietveld refinement to accurately quantify crystalline phases, with corrections for preferred orientation using the March-Dollase model [4–5, 9–16].

XRD analysis revealed key MIC-related phases such as magnetite (Fe $_3$ O $_4$), lepidocrocite (y-FeO(OH)), goethite (α -FeO(OH)), siderite (FeCO $_3$), and various iron sulfides.

The quantitative nature of this approach allows for a detailed understanding of how microbial activity correlates with the development of specific corrosion products [3, 5, 8]. qPCR data, in parallel, provide insights into microbial abundance and community composition, enabling a direct linkage between biological activity and corrosion phase formation.

Rietveld refinement plays a central role in this investigation by enabling precise phase quantification even in complex, multiphase samples. However, due to the influence of preferred orientation diffraction on intensities, the application of the March model was essential for improving accuracy and reliability in quantitative analysis [10-17]. The integration of these methods forms a robust analytical framework for studying mechanisms high-sulfur MIC in environments.

The objectives of this study are as follows:

- 1.To identify and quantify microbial communities responsible for MIC in refinery SRU equipment.
- 2.To characterize corrosion products using quantitative XRD and Rietveld refinement techniques.
- 3.To establish correlations between microbial populations and specific corrosion phases, with an emphasis on SRB and IOB activity.
- 4. To assess the combined utility of qPCR and XRD in elucidating MIC mechanisms for informed corrosion mitigation.

By integrating molecular biology tools with mineralogical characterization, this study offers novel insights into the underlying mechanisms of MIC in sulfur-rich petrochemical environments.

The findings support the development of targeted monitoring and prevention strategies to enhance equipment reliability

and extend operational life in refinery infrastructure [4–5, 20–23].

Experimental Work

investigate the mechanisms microbial-induced corrosion (MIC) in sulfur recovery unit (SRU) equipment, multidisciplinary analytical approach was employed, integrating microbiological and mineralogical techniques. This included the collection and analysis of corrosionassociated sludge samples, followed by microbial community profiling and mineral phase identification using advanced quantitative methods.

Sample Collection and Preliminary Characterization

Sludge samples were collected from key components of the SRU in Plant J-87, specifically from the steam blowdown drum (D-106) and heat exchangers (HE-116 and HE-119), as shown in Figures 1 and 2. These locations were selected due to visible evidence of corrosion and suspected microbial activity. The samples were stored sterile. airtight containers transported under refrigerated conditions to preserve microbial integrity. Prior to analysis, samples were homogenized and sub-divided for microbiological and mineralogical assessments.

Analytical Methods

Microbial Profiling via Quantitative PCR (qPCR)

Quantitative polymerase chain reaction (qPCR) was employed to detect and quantify microbial populations commonly implicated in MIC. Targeted microbial groups included sulfate-reducing bacteria (SRB), methanogens (MET), iron-oxidizing bacteria (IOB), and acid-producing bacteria (APB). DNA was extracted using

standardized protocols optimized for environmental sludge matrices. Specific primers were used for each microbial group, and qPCR amplification was conducted using a real-time thermal cycler. The resulting quantitative data provided insights into microbial abundance and distribution within each sample, forming the basis for correlation with corrosion product formation.

X-Ray Powder Diffraction (XRD) Analysis

The mineralogical composition of corrosion products was characterized using X-ray powder diffraction (XRD). Sludge samples were pretreated to remove organic matter and dried at low temperature to preserve mineral integrity. Subsequently, samples were finely ground to achieve uniform particle size, improving diffraction quality. XRD measurements were performed using a Rigaku Ultima IV diffractometer, operating with Cu-K α radiation under standard scanning conditions. Diffraction patterns were collected over a 2 θ range suitable for identifying corrosion-related crystalline phases.

Maior corrosion products identified included magnetite (Fe₃O₄), lepidocrocite (y-FeO(OH)), goethite $(\alpha-FeO(OH))$, siderite (FeCO₃), and various iron sulfides—all commonly associated with microbial activity in high-sulfur industrial environments [5,18-19].

Quantitative Phase Analysis Using Rietveld Refinement

To achieve precise quantification of corrosion phases, Rietveld refinement was applied to the XRD data using the **General Structure Analysis System (GSAS)** software [14-19,22]. The refinement process included background fitting, unit cell parameter optimization, and peak profile

adjustments. Crucially, the March-Dollase model [10-13] was implemented to correct for preferred orientation effects, which are common in layered or platy corrosion products such as lepidocrocite and goethite.

This refinement enabled accurate determination of the weight percentages of each crystalline phase present in the samples. Such quantitative analysis was critical in correlating the mineralogical data with microbial abundance derived from qPCR.

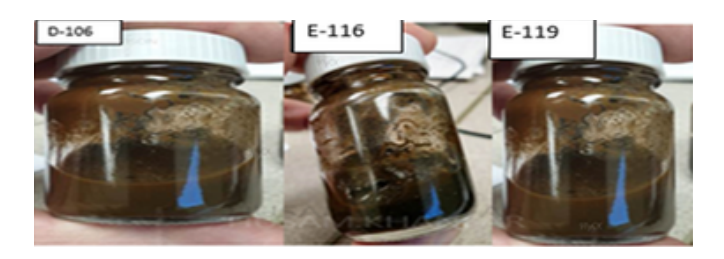


Figure 1. Sludge samples collected from D-106, HE-116, and HE-119 at the sulfur recovery unit of Plant J-87.

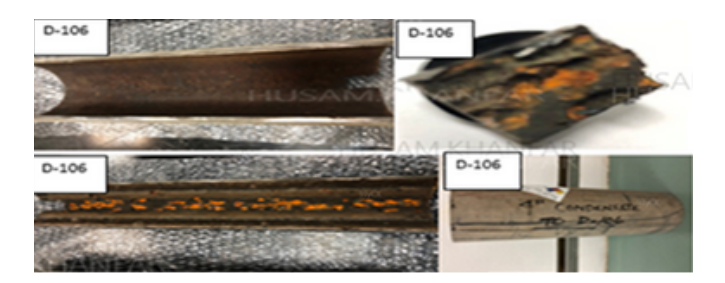


Figure 2. Corroded pipe outlet from the steam blowdown drum (D-106) showing MIC damage

Integration of Microbial and Mineralogical Data

By correlating microbial population data with XRD-based phase quantification, clear relationships between specific microbial groups and their associated corrosion products were established. For instance:

- SRB were strongly linked to the formation of iron sulfides and siderite, confirming their role in anaerobic corrosion pathways.
- **IOB** were associated with the formation

of magnetite, lepidocrocite, and goethite, reflecting their oxidative corrosion influence.

These findings confirm that microbial activity significantly influences the type and extent of corrosion products formed in SRU environments, providing valuable insight into MIC progression.

Conclusion of Experimental Design

This integrated methodology—combining qPCR for microbial community profiling quantitative XRD with and Rietveld refinement for corrosion phase analysis offers а powerful framework understanding MIC in petrochemical environments. It enables direct linkage between biological activity mineralogical outcomes, thus supporting the development of targeted corrosion mitigation strategies in refinery systems.

Table 1. Microbial populations (cells/g) in sludge samples from Plant J-87, as determined by qPCR. BDL: Below Detection Limit

Name	Descri pt-	Quantitative polymerase chain reaction (qPCR) microbial count (cell/g)					
tions	tions	BA	BA SRB MET IOB SRL APB				
D-106	Sludge	1.22	2.73	BDL	2.48		
		x10 ⁶	x10 ³		x10 ⁶	BDL	BDL
E-116		2.07	9.02	1.57x	2.25		
		x10 ⁴	x10 ³	10 ³	x10 ⁴		
E-119		5.76	1.03	3.91x	1.78		
		x10 ⁶	x10 ⁴	104	x10 ⁶		
D-106	Solid	Below the detection limit (BDL))		

Results

1. Microbial Community Analysis via qPCR

Quantitative polymerase chain reaction (qPCR) was employed to assess microbial populations in sludge samples obtained from the steam blowdown drum (D-106) and heat exchangers (HE-116 and HE-119) at Plant J-87. The results revealed microbial loads up to 10⁶ cells/g, with significant populations of iron-oxidizing bacteria (IOB), sulfate-reducing bacteria (SRB), and

acid-producing bacteria (APB) (Table 1). Notably, no MIC-related microbes were detected in the corroded metal sample from the failed D-106 pipe, indicating a limited microbial contribution to corrosion at the metal interface at the time of sampling.

2. Thermogravimetric Analysis (TGA)

Thermogravimetric analysis revealed weight losses indicative of organic and volatile compound content within the sludge. Weight loss values at 900 °C were 10.0%, 17.0%, and 16.0% for samples from D-106, HE-116, and HE-119, respectively, confirming a mixture of organic matter and mineral phases (Table 2, Figure 3).

Table 2. TGA results showing weight loss and residual content in sludge samples.

Sample name	Loss at 200°C	Loss at 600°C	TWL @ 900°C	wt% of residual @ 900°C
D-106	6	4	10	90
HE-116	8	8	17	83
HE-119	7	8	16	84

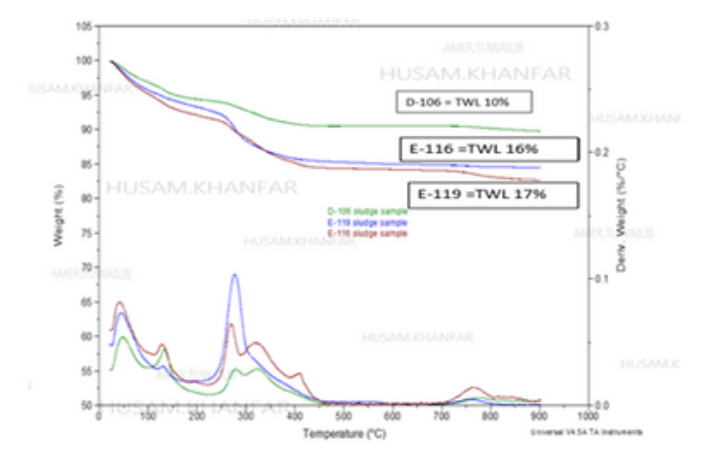


Figure 3. Overlaid TGA profiles of sludge from D-106, HE-116, and HE-119 at Plant J-87.

3. Gas Chromatography–Mass Spectrometry (GC-MS)

GC-MS analysis of hexane-extracted organics from the sludge revealed a wide hydrocarbon range (C_{10} – C_{30}), with a bimodal distribution in D-106 and HE-116 samples. No aromatic hydrocarbons were detected, suggesting the hydrocarbons were primaril

primarily aliphatic and likely derived from process fluids or bio-origin (Figure 4).

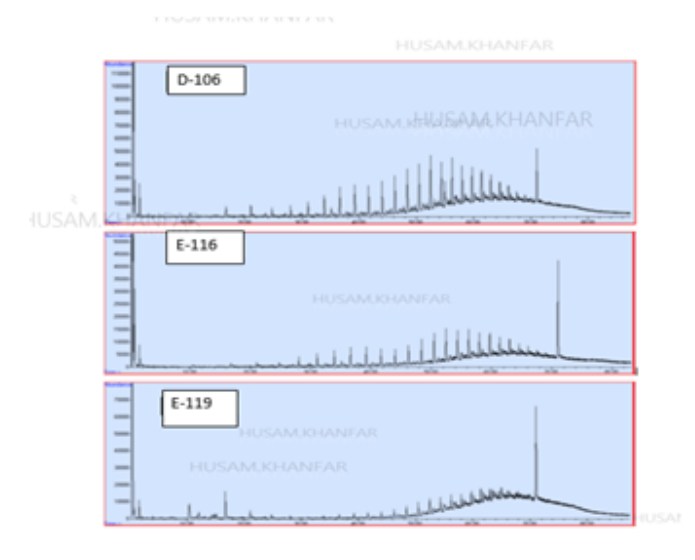


Figure 4. GC-MS chromatogram of extracted hydrocarbons from sludge samples (D-106, HE-116, HE-119).

4. Quantitative Mineral Phase Identification via XRD and Rietveld Refinement

diffraction (XRD), followed X-ray Rietveld refinement with preferred orientation correction (March-Dollase model). identified several crystalline corrosion products in the sludge samples. These included magnetite (Fe_3O_4) . lepidocrocite (y-FeO(OH)), goethite (α-FeO(OH)). siderite (FeCO₃), and trace secondary minerals such as vivanite, dolomite, and calcite.

Table 3. Quantitative phase composition of sludge samples determined via Rietveld refinement.

Identified Phases	Rietveld Phase Composition (wt%) Results					
	D-106	HE-116	HE-119	D-106		
Magnetite [Fe ₃ O ₄]	80	91	50	90		
Lepidocrocite	2	3	46	-		
[FeO(OH)]						
Goethite	-	6	4	-		
[FeO(OH)]						
Vivanite	Trace					
$[\mathrm{Fe_3(PO_4)(H_2O)_8}]$						
Siderite	8	-	-	10		
Goryainovite	Trace	-	-	-		
[Ca ₂ (PO ₄)Cl]						
Dolomite	1	-	-	-		
[CaMg(CO3)2]						
Quartz [SiO2]		Tra	ce			
Calcite [CaCO3]	9 Trace					

5. Correlation Between Microbial Activity and Mineral Phases

The integration of microbial and mineralogical data highlighted distinct correlations between specific microbial groups and iron-based corrosion products:

- SRB activity promotes hydrogen sulfide generation, leading to iron sulfide and siderite formation.
- IOB facilitate the oxidative transformation of iron, resulting in magnetite, lepidocrocite, and goethite.
- APB contribute by acidifying the local microenvironment, accelerating metal dissolution and mineral transformation.

The dominance of magnetite across all samples, particularly in HE-116 (91%), suggests intense IOB activity and a relatively stable redox regime. In contrast, the elevated lepidocrocite in HE-119 (46%) points to fluctuating oxidation-reduction conditions, likely influenced by biofilm dynamics and pH variability.

Key Insights and Interpretations

- MIC in SRU sludge is primarily driven by the activity of SRB, IOB, and APB.
- Microbial metabolism facilitates the formation of iron oxides and carbonates, particularly magnetite, lepidocrocite, and siderite.
- Biofilm formation on metallic surfaces enhances corrosion by creating localized electrochemical gradients.
- Fluctuating environmental conditions, such as pH and oxygen availability, strongly influence microbial community composition and corrosion pathways.
- The absence of detectable microbes in the failed D-106 pipe metal suggests post-corrosion inactivity or environmental shifts unfavorable to microbial survival.

Discussion

This study investigated sludge deposits collected from pipelines D-106, HE-116, and HE-119 at Plant J-87 to elucidate the mechanisms of microbiologically influenced corrosion (MIC) and their association with the mineralogical composition of corrosion products. Through a multidisciplinary approach combining microbial characterization and X-ray diffraction (XRD) analysis, critical insights were gained into the spatial variability and causative factors underlying MIC in refinery pipeline systems.

Microbial Activity and Localized Corrosion Phenomena

Microbiological analysis revealed the presence of key corrosion-related microbial taxa, including sulfate-reducing bacteria (SRB), iron-oxidizing bacteria (IOB), and acid-producing bacteria (APB). These microorganisms are widely recognized for their role in promoting MIC via metabolic by-products that alter local electrochemical conditions. In particular, SRB reduce sulfate to hydrogen sulfide (H₂S), which reacts with ferrous iron to precipitate iron sulfide phases such as pyrite (FeS₂) and marcasite (FeS₂). These minerals are associated with aggressive, localized corrosion processes.

Notably, while these microorganisms were prevalent in several sludge samples, they were absent in the critical failure zone of pipeline D-106. This suggests that MIC may not have been the primary failure mechanism in that section. Instead, the corrosion observed there may have been influenced by non-biological factors such as oxygen ingress, moisture accumulation, or the presence of corrosive chemical species. This observation underscores the site-specific nature of MIC and highlights the

necessity of localized assessment rather than system-wide generalizations when diagnosing corrosion mechanisms in complex refinery systems.

Mineralogical Signatures of MIC: Insights from XRD

XRD analysis. enhanced bv Rietveld refinement, enabled detailed identification and quantification of crystalline corrosion products across different pipeline sections. In MIC-affected regions, corrosion scales predominantly contained iron sulfides specifically pvrite and marcasite consistent with SRB-driven biocorrosion. In contrast, samples from less biologically active zones were dominated by iron oxides, including magnetite (Fe₃O₄), goethite (αand lepidocrocite FeOOH), (y-FeOOH). These oxides are indicative of abiotic corrosion pathways typically associated with environments oxygenated atmospheric exposure.

This mineralogical differentiation serves as robust diagnostic criterion distinguishing MIC from abiotic corrosion. The presence of sulfur-rich phases in offers direct evidence particular microbial involvement and complements microbiological data to provide a more holistic understanding of corrosion mechanisms.

Integrating Microbial and Mineralogical Diagnostics

The combined use of microbial profiling and XRD-based mineral analysis proved effective in correlating microbial presence with the composition and distribution of corrosion products. While microbial assays confirmed the existence of SRB and other MIC-related organisms, the detection of specific iron sulfide minerals via XRD provided definitive evidence of their

corrosive impact. This integrated methodology strengthens the reliability of MIC assessments and enhances the resolution with which corrosion origins can be pinpointed.

Engineering and Operational Implications

The identification of iron sulfide phases in association with SRB presence reinforces the critical role of MIC in refinery infrastructure degradation. Iron sulfides not only indicate microbial activity but also signify zones of intensified, localized corrosion that can compromise pipeline integrity. These findings align with previous work by Wuhaib et al. [23], who emphasized persistence of diverse microbial communities — including SRB, IOB, methanogens—in crude oil and sludge environments. Such microbial consortia are known to form biofilms and generate corrosive microenvironments that challenge conventional corrosion control methods.

Given the demonstrated correlation between microbial activity and mineralogical signatures of corrosion, there is a clear imperative to incorporate regular microbial monitoring into refinery maintenance programs. In particular, the presence of complex corrosion products such as pyrrhotite, lepidocrocite, goethite highlights the multifactorial nature of MIC and calls for a more nuanced approach to corrosion diagnostics and mitigation.

Recommendations for MIC Management and Prevention

Based on the outcomes of this study and corroborating literature, a proactive, data-driven corrosion management strategy is strongly recommended. Quarterly sampling of water, hydrocarbon fluids, and solid

residues from key upstream and midstream locations should be implemented. Concurrent microbial assessments—utilizing both culture-based and molecular techniques—can facilitate early detection of MIC risk factors and support timely intervention.

Moreover, the integration of geochemical and mineralogical data with microbial profiles can guide the selection and optimization of targeted mitigation strategies, including biocide application and environmental control (e.g., oxygen and moisture exclusion). Such multidisciplinary diagnostics not only improve MIC prediction but also enhance the resilience and longevity of refinery pipeline systems.

Conclusion

This study explored the role of microbiologically influenced corrosion (MIC) in refinery systems, emphasizing the contribution of sulfate-reducing bacteria (SRB) and the utility of X-ray diffraction (XRD) techniques for corrosion product characterization. The principal findings are summarized as follows:

Microbial Profiling: Sludge samples collected from pipelines exhibited moderate to high microbial loads, with the detection of SRB, methanogens, and iron-oxidizing bacteria (IOB) — all known contributors to MIC. Notably, these organisms were absent in the failed section of pipeline D-106, suggesting that microbial activity was not the primary driver of corrosion at that location.

Spectroscopic Analysis:

Thermogravimetric analysis (TGA) revealed weight loss associated with moisture, hydrocarbons, and polymeric residues, with inorganic crystalline

phases remaining as residuals. Gas chromatography-mass spectrometry (GC-MS) detected components resembling lubricating oils or greases but showed no presence of crude oil, indicating the sludge's processed origin.

 Mineralogical Characterization: XRD analysis, supported by Rietveld refinement. identified predominant corrosion products as iron oxides namely magnetite (Fe₃O₄), lepidocrocite (y-FeOOH), and goethite (α -FeOOH). In areas affected by microbial activity, iron sulfide minerals such as pyrite (FeS₂) and marcasite were also present, strongly implicating SRB in localized and more aggressive corrosion mechanisms.

These results confirm the significant role of microbial processes - particularly those mediated by SRB—in promoting formation of corrosive iron sulfide scales. The combined use of microbiological assays and mineralogical techniques, especially XRD with Rietveld refinement, proved effective in distinguishing microbial versus abiotic corrosion environments. This offers valuable integrated approach diagnostic insight for corrosion risk management in industrial settings.

Outlook

To build upon the current findings and enhance corrosion control strategies in refinery operations, future research should adopt a more integrated and high-resolution investigative framework. Key recommendations include:

 Advanced Microbial Characterization: Incorporate molecular diagnostics such as quantitative polymerase chain reaction (qPCR),metagenomics, and high-throughput sequencing to more precisely identify and quantify microbial populations involved in MIC.

- Comprehensive Sampling Regimes: Implement routine, site-specific sampling of sludge, water, and deposits across operational units. Pair microbial data with mineralogical analysis using high-resolution X-ray powder diffraction and Rietveld refinement for phase-specific insights.
- Real-Time Monitoring and Predictive Control: Integrate real-time microbial monitoring systems into corrosion management protocols to enable early detection of MIC onset and guide timely mitigation interventions, including biocide application or environmental modification.
- Material Innovation and Coatings:
 Pursue the development and deployment of MIC-resistant materials
 — such as high-performance alloys and protective coatings—tailored to microbial and chemical conditions prevalent in refinery environments.
- Interdisciplinary **Collaboration:** multidisciplinary approach involving materials microbiology, science. corrosion engineering. and data analytics will be essential addressing the complex and evolving challenges posed by MIC. collaboration will support the design of predictive models, the optimization of treatment strategies. and the advancement sustainable of infrastructure management in industrial systems.

In conclusion, integrating microbiological surveillance with advanced materials characterization offers a promising pathway for reducing MIC-related failures

and improving asset longevity in the energy and petrochemical sectors.

Acknowledgments

authors sincerely thank the The management of Saudi Aramco for granting permission to publish this work. Special appreciation is extended to the professionals and technicians of the Research and Analytical Services Department (RASD) for their technical and valuable support contributions throughout the study. The authors also gratefully acknowledge the anonymous reviewer and the Editor of Journal of Chemical Research and Innovation Society (JCRIS) for their insightful comments and constructive suggestions, significantly enhanced the quality and clarity of this manuscript.

References

- 1.G.P.V. Dalmora, E.P.B. Filho, A.A.M. Maraschin Conterato, W.S. Roso, A.C.E. Pereira, L.L. Dettmer, Methods of corrosion prevention for steel in marine environments: A review. Results Surf. Interfaces, 18 (2025) 100430. https://doi.org/10.1016/j.rsurfi.2025.100430
- 2.X. Sun, O.H.W. Way, J. Xie, X. Li, Biomineralization to prevent microbially induced corrosion on concrete for sustainable marine infrastructure. Environ. Sci. Technol. 58 (2024) 522–533.
 - https://doi.org/10.1021/acs.est.3c04680
- 3.H.S. Khanfar, H. Sitepu, X. Zhu, Use of microbiological, geochemical, and X-ray diffraction techniques to support the autopsy of reverse osmosis membrane from a Saudi Aramco gas plant. AMPP ME Corrosion Conf. Expo, (2023) AMPP-MECC-2023-20019.

- T.H. Yen, A.P. Dang, D. Cozzolino, D. Dinh, K.B. et al., Analytical characterization of material corrosion by biofilms. J. Bio-Tribo-Corrosion 8(2) (2022). https://doi.org/10.1007/s40735-022-00648-2
- 5. H.S. Khanfar, H. Sitepu, A lab case study of microbiologically influenced corrosion and Rietveld quantitative phase analysis of X-ray powder diffraction data of deposits from refinery. ACS Omega 6 (2021) 11822–11831.
 - https://doi.org/10.1021/acsomega.0c047
- H. Choi et al., Microbial influence on corrosion of steel in sulfate-reducing environments. Corros. Sci. 163 (2020) 108179.
- P. Kannan, S.S. Su, M.S. Mannan, H. Castaneda, S.A. Vaddiraju, Review of characterization and quantification tools for MIC in the oil and gas industry: Current and future trends. Ind. Eng. Chem. Res. 57 (2018) 13895–13922. https://doi.org/10.1021/acs.iecr.8b02211
- 8. G.S. Dhillon et al., Microbial corrosion and its impact on material integrity in oil and gas systems. Front. Microbiol. 8 (2017) 1159.
- G. Tian et al., Quantitative phase analysis of corrosion products in microbial induced corrosion environments. J. Appl. Microbiol. 127 (2019) 230–240.
- W.A. Dollase, Correction of intensities for preferred orientation in powder diffractometry: Application of the March model. J. Appl. Cryst. 19 (1986) 267–272.
 - https://doi.org/10.1107/S002188988608 9458

- 11. D.Y. Li, B.H. O'Connor, G.I.D. Roach, J.B. Cornell, Use of X-ray powder diffraction Rietveld pattern-fitting for characterising preferred orientation in gibbsite. Powder Diffr. 5(2) (1990) 79–85.
- 12. B.H. O'Connor, D.Y. Li, H. Sitepu, Strategies for preferred orientation corrections in X-ray powder diffraction using line intensity ratios. Adv. X-ray Anal. 34 (1991) 409–415.
- 13. B.H. O'Connor, D.Y. Li, H. Sitepu, Texture characterization in X-ray powder diffraction using the March formula. Adv. X-ray Anal. 35 (1992) 277–283.
- 14. H. Sitepu, Assessment of preferred orientation with neutron powder diffraction data. J. Appl. Cryst. 35 (2002) 274–277.
- 15. H. Sitepu, Texture and structural refinement using neutron diffraction data from molybdite (MoO₃) and calcite (CaCO₃) powders and a Ni-rich Ni_{50·7}Ti_{49·3} alloy. Powder Diffr. 24 (2009) 315–326.
- 16. H. Sitepu, B.H. O'Connor, D.Y. Li, Comparative evaluation of the March and generalized spherical harmonic preferred orientation models using Xray diffraction data. J. Appl. Cryst. 38 (2005) 158–167.
- 17. H. Sitepu, Rietveld phase analysis of deposits formed at different locations within electric submersible pumps. Adv. X-Ray Anal. 63 (2020) 28–42.
- H. Sitepu, N.M. AlYami, I.M. Al-Zahrani, Quantitative Rietveld analysis of crystalline deposits to support failure investigation. Adv. X-Ray Anal.67 (2024) 103–115.

- 19. H. Sitepu, N.M. AlYami, I.M. Al-Zahrani, Texture and structural refinement and quantitative Rietveld analysis of crystalline deposits. Powder Diffr.40 (2025) 7–20.
- 20. H.J. Bunge, Preferred orientation in polycrystalline materials. Adv. X-ray Anal. 25 (1982) 181–185.
- 21. N.C. Popa, Refinement of crystallographic texture by the generalized spherical harmonics approach. J. Appl. Cryst. 25 (1992) 611–616.

- 22. R.B. Von Dreele, Quantitative texture analysis by Rietveld refinement. J. Appl. Cryst. 30 (1997) 517–525.
- A.S. Al-Wuhaib, H. Sitepu, H.S. Khanfar, 23. W.A. Algozeeb, A.M. Wade, Microbial and compositional analyses of oil and sludge from crude pipelines. ISOMOS Book Chapter (Accepted, 2025).

Author

Dr. Husam S. Khanfar is a Senior Research Scientist at Saudi Aramco's Research and Analytical Services Department. He holds a Ph.D. and M.S. from the Arab University of Bahrain, where his research focused on microbiology-induced corrosion, and a B.Sc. from the University of Jordan. Dr. Khanfar specializes in materials characterization to support failure analysis investigations and catalyst development. He has authored and co-authored over 20 journal articles.

Dr. Husin Sitepu, recently retired from Saudi Aramco after 16 years, is an expert in applied crystallography and diffraction science. His research focused on advanced materials characterization using XRF, XRD, and the Rietveld method, supporting catalyst development, QA/QC, and failure analysis. With 70+ publications, he holds a Ph.D. in Physics and is active in ICDD, IUCr, and NSSA.

Noha S. Al-Shihri is an Associate Scientist at Saudi Aramco's Research and Analytical Services Department. She holds an M.Sc. degree in Chemistry from Rochester Institute of Technology, Rochester, New York, USA. Her expertise encompasses materials characterization using FTIR, TGA, and Raman spectroscopy to support research and failure analysis investigations. She has presented papers at reputable conferences and holds several patents.

Dr. Mona AlDossary is Lead Lab Scientist at Saudi Aramco's RASD. She earned her Ph.D. and M.Sc. in Chemistry from KAUST. focusing on advanced materials for solar cell applications, and a B.Sc. from King Faisal University. With expertise in materials characterization. she has published over 10 papers and holds five patents in materials science and renewable energy.

Dr. Xiangyang Zhu has over 25 years of experience in teaching, R&D, and technical services in academia, research institute, and energy industries. He is a pioneer in introducing modern molecular microbiology technologies into oil and gas industry. Currently he is a Research Science Consultant at Research and Analytical Services Department of Saudi Aramco.

Ibrahim M. Al-Zhahrani is a Senior Research Consultant at Saudi Aramco's RASD. He earned his Ph.D. and M.Sc. from KFUPM and a B.Sc. from King Saud University, specializing in catalyst synthesis and characterization using TGA, FTIR, and Raman spectroscopy. With expertise in materials characterization, he has published 20+ papers and holds over 10 U.S. patents.

Place Your Advertisement Here

Contact us at editorial@cris.org.sa

Recent Advances in Sustainable Polycarbonate Synthesis, Recyclability, and Emerging Applications

Najd A. Alhussain¹, Florian Stadler²*

¹Applied Research Center for Environment and Marine Studies (ARC-EMS), Research & Innovation, King Fahd University of Petroleum and Minerals (KFUPM), 31261,

Dhahran, Saudi Arabia

² Department of Chemical Engineering, King Fahd University of Petroleum and Minerals, 31261, Dhahran, Saudi Arabia

*f.stadler@kfupm.edu.sa

Abstract

Polycarbonate (PC) versatile is а engineering thermoplastic known for its optical clarity, thermal stability, chemical resistance, and high impact strength. These qualities make it a key material across industries such as automotive, electronics, biomedical. and packaging. However, traditional PC production relies hazardous monomers like bisphenol A (BPA) and phosgene, which raise environmental and health concerns due to solvent use and toxic byproducts. This review highlights recent advances in sustainable polycarbonate production, focusing on ecofriendly approaches such as using carbon dioxide as a raw material and developing green synthesis methods from renewable bio-based monomers like isosorbide and fatty acids. It also explores innovative catalytic and polymerization techniques, including machine learning-assisted catalyst design, which help accelerate development and improve polymer performance. Additionally. progress chemical recycling and upcycling methods is discussed, supporting circular economy models for polycarbonates. Finally, the review covers the expanding applications of polycarbonates across various green industries. Overall, this comprehensive overview emphasizes the potential of green

polycarbonates to transform plastics manufacturing toward sustainability without compromising quality or performance.

Introduction

Engineering thermoplastics such polycarbonate (PC) are renowned for their exceptional mechanical strength optical transparency, making them indispensable in wide а range applications. PC's high impact resistance, structural integrity, and clarity have established its importance across various industrial sectors.[1] Polycarbonate (PC) exhibits remarkable chemical resistance, cost-effectiveness, thermal stability, and stiffness, attributes that contribute to its versatility [2]. Additionally, its ultraviolet resistance and lightweight nature make it suitable for diverse applications. Notably, PC has been employed in fields such as additive manufacturing [3], automotive engineering [4], biomedical devices [5], electromagnetic optical systems [6], shielding [7], and food packaging [8]. As illustrated in Figure 1a and 1b, traditional PC is synthesized via the polycondensation of bisphenol A (BPA) with diphenyl carbonate (DPC) or through the reaction of BPA with phosgene [9].

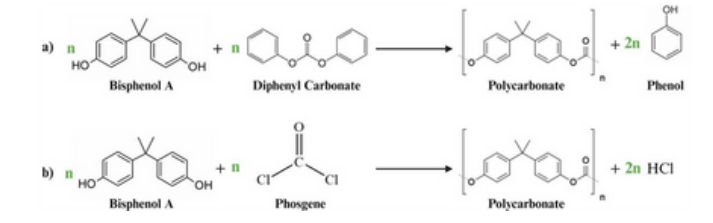


Figure 1. A schematic synthesis of conventional polycarbonate, a) from the reaction of BPA and DPC, and b) from the reaction of BPA and Phosgene.

Conventional polycarbonate (PC) synthesis methods often involve substantial solvent usage and generate significant effluent, raising environmental concerns. Consequently, the development environmentally benign alternatives has garnered considerable attention. One such approach entails the utilization of carbon dioxide (CO₂) as a raw material in conjunction with diphenyl carbonate (DPC) for PC production, offering a more sustainable pathway. In addition to CO₂based methods, the synthesis of PCs from bio-based monomers presents a promising avenue for producing performanceenhanced and environmentally friendly plastics. Monomers such as limonene oxide and isosorbide, derived from terpene and sugar sources, respectively, have been explored for this purpose. Comprehensive reviews [10-12] have thoroughly examined the sustainability of bio-based monomers and highlighted the advantageous properties of the resulting polymers. The pursuit of eco-friendly, cost-effective, and sustainable PC production methods has gained significant momentum in recent years. The focus is directed towards upcycling strategies, specifically the efficient conversion of carbon dioxide (CO₂) and biomass into PC, which theoretically presents a lower environmental burden compared to traditional petroleum-based monomers. Recent innovations harness machine learning to accelerate the design

of green PCs through linking epoxide comonomer structure, catalysts, polymerization conditions, and use this dataset to train machine-learning models that predict molecular weight, polymer vield. and selectivity. The Al-driven approach identified previously overlooked catalyst-monomer combinations suggested optimal reaction windows, which subsequently were validated experimentally [13]. Such data-centric strategies significantly shorten development cycles, reduce experimental waste, and can be integrated into highthroughput synthesis platforms to rapidly sustainable advance polycarbonate production.

This review provides a comprehensive overview of recent advances in sustainable polycarbonate synthesis, with particular emphasis on CO₂-based and bio-derived monomers. It critically evaluates the environmental and performance advantages of green polycarbonates, examines strategies of recyclability, and highlights their broad application potential across diverse industries.

PROPERTIES OF GREEN POLYCARBONATE

Polycarbonate is renowned for its high impact resistance and commendable tensile strength, attributes that enhance its applicability across various domains [14]. Its inherent optical transparency further extends its utility to optical applications. Recent advancements have explored the integration of bio-based precursors, such as silicone blocks, into the PC matrix. This modification has been shown to ameliorate yellowing and enhance ductility, thereby extending the material's service life in both optical and mechanical contexts [15,16].

The presence of chemically active ester and carbonate groups within the PC structure renders it amenable to chemical recycling processes. Innovative methodologies, such solventand catalyst-free as mechanochemical methanolysis. demonstrated efficacy in depolymerizing PC, facilitating the recovery of monomeric constituents [1]. Furthermore. incorporation of thermally conductive fillers. including spherical alumina particles, has been shown to significantly augment the thermal conductivity of PC composites while preserving their excellent electrical insulation properties [17].

In summary, polycarbonate emerges as a robust material with substantial potential in the realm of high-performance, sustainable applications. Its UV resistance, electrical insulating capability, and enhanced thermal conductivity underscore its attractiveness for engineering applications. A comprehensive overview of the diverse properties of green polycarbonates is presented in Figure 2.



Figure 2. Properties of Green Polycarbonate.

Synthesis of Green Polycarbonate

The green synthesis of polycarbonates (PCs) has garnered considerable attention

in recent years. Renewable resources, particularly biomass-derived monomers. have been employed to produce sustainable example, PCs. For vanillin-based poly(acetal-carbonates) have developed for PC applications [18], and fatty acid-derived polymers have also been utilized in PC synthesis. Sugar derivatives such as isosorbide have led to the creation polv(isosorbide carbonate). which exhibits remarkable properties [19]. In addition to bio-based sources, carbon dioxide (CO₂) has emerged as a promising monomer for sustainable PC production. Several studies have reported the successful synthesis of PC-based polymers including poly(trimethylene carbonate), poly(propylene carbonate), and poly(etherco-carbonate-co-acetal) — demonstrating outstanding mechanical and properties [20-22]. Figure 3 illustrates the primary sources utilized in the synthesis of green PCs.

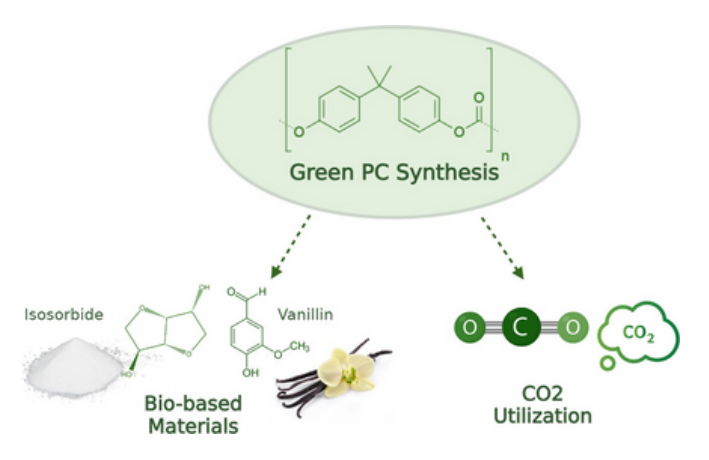


Figure 3. Sources of Green Polycarbonate synthesis.

BIOBASED POLYCARBONATE

In recent years, the exploration of bio-based alternatives to bisphenol A (BPA) monomers has garnered significant attention in the pursuit of more sustainable polycarbonate (PC) materials [23,24] Notably, sugarderived compounds such as poly(isosorbide carbonate)) (PIC) have been investigated for their potential to enhance the properties

of PCs [25].]. Additionally, monomers derived from lignin, terpenes, and fatty acids have been explored as renewable feedstocks for PC synthesis [23]. A schematic representation of these biobased monomers is depicted in Figure 4.

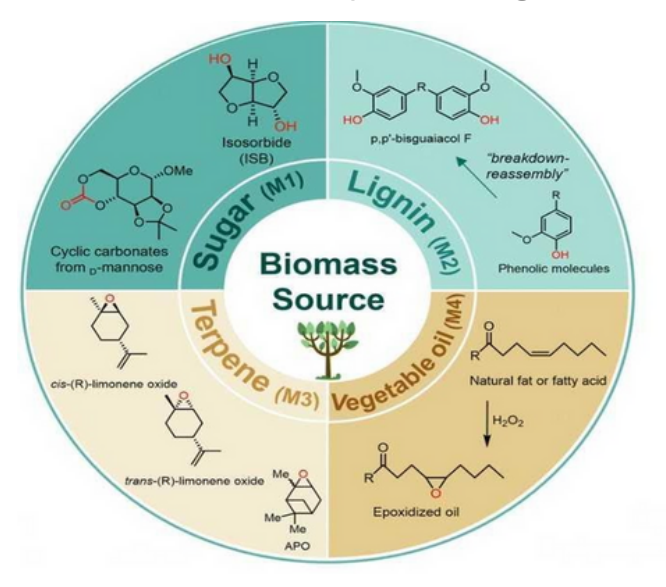


Figure 4. A schematic of bio-based monomers for PCs synthesis. [23].

Bio-based synthesis routes not only reduce dependence on toxic resources but also enable the incorporation of renewable feedstocks. Some recent studies on biobased PCs are summarized in Table 1. Recent work also demonstrates synergy between isosorbide-based polycarbonates and renewable fillers such as nanocellulose. A Korean research team reported that surface-modified incorporating nanocellulose into an isosorbide-rich PC matrix not only improved tensile strength and thermal stability but also enhanced barrier performance against moisture and This bio gases. composite retained and excellent transparency exhibited reduced brittleness, making it suitable for optical and food-contact applications. [26] Furthermore, novel eco-friendly adhesive formulations using isosorbide PC as the base resin have shown high adhesion strength on metals, glass, and certain polymers without requiring hazardous

solvents, expanding the functional scope of green PCs into bonding and coating technologies.

Table 1. A literature reviewon PCs synthesis from variousbiobased materials.

Biobased source	Monomers	Polymer Composite	Polymerization technique	Properties	Ref
Diether anthraquinone	poly (isosorbide carbonate)	Poly (ISB-co-DAQ carbonate)	copolymerization process with catalyst	Excellent thermal, mechanical, and hydrophobicity. Potential for optical applications.	[6]
Vanillin	Divanillin carbonate (DVC) and pentaerythritol (PE), bis-spiro phenol (BSP), and diphenyl carbonate (DPC)	Poly(acetal-carbonates)	Palatalization and polycondensation	High glass transition temperatures (Tg) .	[18]
Sorbitol Isosorbide (ISB)	Isosorbide	Poly(isosorbide carbonate) (PIC)	Transesterification of DPC and ISB	High impact strength and excellent transparency	[27]
Cellulose, starch.	isosorbide (IS) and the semirigid isoidide-2,5- dimethanol (IIDML)	poly(isosorbide carbonate-co- isoidide- 2,5-dimethylene carbonate)	Melt polymerization	High $T_{\mathcal{G}}$,high tensile strength, and high elongation.	[28
Fatty acid	Fatty acid epoxides and carbon dioxide.	terpolymeric compositions	Catalytic ring-opening copolymerization.	Improve the mechanical and adsorption properties of castor oil-based polyurethane gels.	[19]
Sugar (ISB)	Isosorbide and diphenyl carbonate	Isosorbide-based copolycarbonate	Efficient catalyst and copolymerization strategy.	Excellent catalytic activity. High molecular weight	[16]
Eugenol	Eugenol epoxide (EuO), propylene oxide (PO), and CO2	polymonothiocarbonates	Terpolymerization cycloaddition with catalyst	Increase in the Tg values with increase in the eugenol epoxide proportion in the terpolymer	[29]

CO₂ UTILIZATION IN POLYCARBONATE PRODUCTION

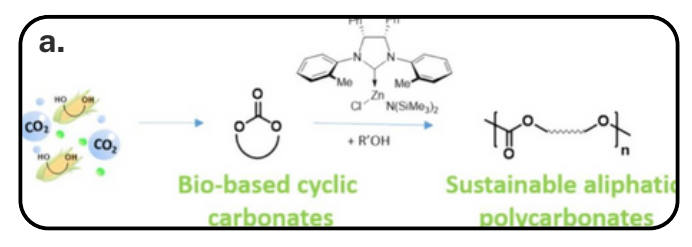
The utilization of carbon dioxide (CO_2) as a comonomer in polycarbonate (PC) synthesis has garnered significant attention from both industrial and academic sectors, serving as a foundation for replacing petroleum-based materials and advancing sustainable development [30]. This interest has spurred extensive research into the fabrication of CO_2 -based polymers to meet the pressing demand for more sustainable materials [31].

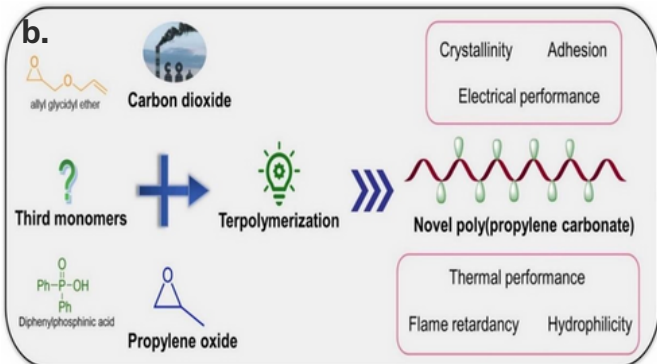
Numerous studies have explored the synthesis of polycarbonates using CO₂ as a core monomer. For instance. poly(trimethylene carbonate) was via synthesized ring-opening polymerization, initiating a green process that commenced with renewable starting materials, including CO₂ and 1,3-diols. This approach achieved a high turnover frequency (TOF) of up to 760 h^{-1} [20], as shown in Figure 5a. A recent study explored the copolymerization of carbon dioxide and propylene oxide (PO) to synthesize biodegradable poly(propylene carbonate) (PPC). This process utilizes excess CO₂, contributing to sustainable polymer production. The resulting PPC exhibits environmentally friendly

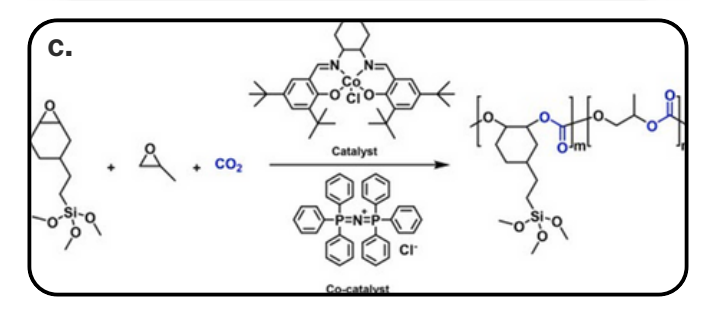
material for various applications. [21] The overall reaction scheme leading to the formation of star-shaped PPC is illustrated in **Figure 5 b.** In the context of the direct copolymerization of epoxides and carbon dioxide (CO₂), A new study provided a comprehensive overview of catalytic strategies that have been employed to enhance the formation of cyclic carbonates. [32] Their discussion centers on the development of catalysts for the direct copolymerization of epoxides with CO₂, as well as the copolymerization of diols with CO₂ for the preparation of polycarbonates. Furthermore. Α novel CO₂-based polycarbonate terpolymer was synthesized via the copolymerization of propylene oxide (PO), CO₂, and an epoxy-functionalized specifically silane. [2-(3.4epoxycyclohexyl)ethyl]trimethoxysilane (TMSO). [33] The reaction pathway for this terpolymerization is illustrated in Figure 5c. A recent study reported a novel approach synthesizing low molar polycarbonate diols through the acidcatalyzed degradation of high molar mass poly(ether-co-carbonate-co-acetal) terpolymers. These terpolymers were synthesized via the terpolymerization of propylene oxide (PO), o-phthalaldehyde (OPA), and carbon dioxide (CO₂), employing triethyl borane (TEB) as an activator and an onium salt as an initiator. The incorporation of labile acetal linkages within the polymer backbone allowed for subsequent cleavage under mild acidic conditions, yielding α,ω polycarbonate diols [22]. Notably, the OPA released during hydrolysis efficiently recovered and recycled further polymerization processes. experimental setup and reaction pathway are illustrated in **Figure 5d.**

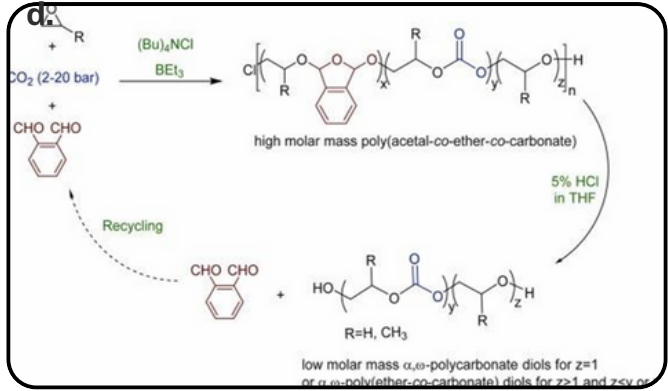
characteristics, making it a promising

solvents, expanding the functional scope of green PCs into bonding and coating technologies.









Figureure 5 a). Polytrimethylene synthesisby using CO2 and diols as a monomer.[20] **b)** The synthesis of poly (propylene carbonate) via CO2 and PO reaction[21]. **c)** Terpolymerization of TMSO/PO/CO2. [33]. **d)** Terpolymerization of PO with CO₂ and OPA for low molar mass polycarbonate and poly(ether-co-carbonate) diols [22].

Polycarbonate Recyclability

Plastic waste upcycling refers to the transformation of plastic waste into materials or products of higher quality or

value, without diminishing the material's integrity [34]. This approach contrasts with traditional recycling methods, which often degrade the material's quality. Upcycling contributes to sustainable development by reducing reliance on virgin resources and minimizing environmental impact.

Beyond conventional solvent and densitybased recovery, researchers are exploring co-upcycling strategies that convert PC waste directly into high-value materials. In 2025. а studv demonstrated simultaneous depolymerization of waste polycarbonate and polyethylene terephthalate (PET) in the presence of a metal-free ionic liquid catalyst under mild methanolysis conditions. This approach yielded high-purity bisphenol A and dimethyl terephthalate in the same reactor, which were then co-polycondensed to produce high-performance polyarylate with a glass transition temperature above 200 °C and excellent optical transmittance. [35] Such integrated processes offer economic and environmental advantages by avoiding separate recycling streams and enabling direct production of value-added engineering plastics.

In the realm of polycarbonate (PC) recycling, a study developed a green and sustainable process for recovering PC from electronic waste. Their methodology involved a two-step approach:

First, density separation was employed using saltwater solutions to segregate heterogeneous polymers present in electronic waste, effectively isolating PC from other materials. This method leverages the differences in density among various polymers, allowing for efficient separation.

Second, solvent-based recycling was conducted utilizing Hansen Solubility

Parameter (HSP) theory to identify suitable solvents and antisolvents for PC dissolution and recovery. The study found that Nmethyl-2-pyrrolidone (NMP) and dichloromethane (DCM) could completely dissolve waste PC. Subsequently, water was identified as the most effective antisolvent when used with NMP, achieving a precipitated yield of approximately 90%. [36] This process not only facilitates the efficient recovery of PC but also aligns with environmental sustainability goals reducing the need for virgin materials and hazardous minimizing waste. experimental design and process flow are illustrated in Figure 6.a.

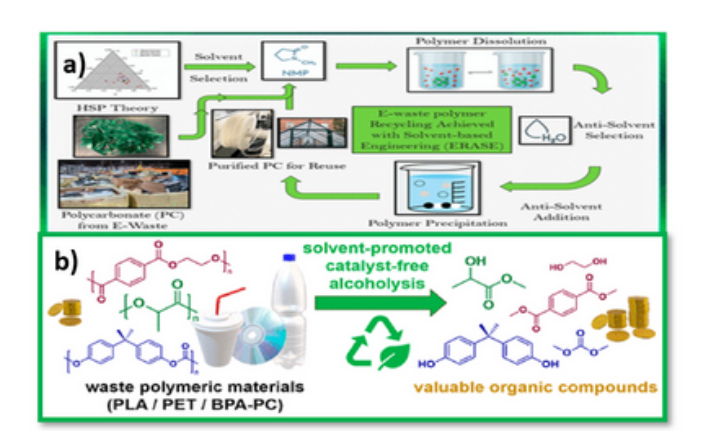


Figure 6. a) Recycling of polycarbonate (PC) from electronic waste plastics [36], b) Catalyst-Free technique for plastic recycling. [37]

Polyester and polycarbonate materials can be depolymerized in a catalyst-free process to produce small organic molecules by alcoholysis (see also, depolymerization). [37] However, several polar organic solvents can depolymerize plastics with very high efficiency even without catalyst processing. By using these polar solvents, alcoholysis can efficiently degrade polymer resinsand commercially available products. So, **Figure 6.b** is for clarification of the plastic polymers regeneration in the catalyst-free process.

Complementary to physical recycling, chemical depolymerization with benign catalysts has advanced rapidly. A 2024 mini-review summarized state-of-the-art catalytic systems for poly(bisphenol A carbonate) glycolysis, including magnesium acetate, zinc acetate, and ionic liquids, which achieve near-quantitative recovery of

bisphenol A and cyclic carbonates under relatively low temperatures (120–180 °C). Process intensification techniques such as reactive extrusion and microwave-assisted depolymerization further reduce energy input and reaction time.[38] These developments could enable scalable, closed-loop recycling systems for both fossil- and bio-based PCs.

POLYCARBONATE APPLICATIONS

PCs engineering are amorphous thermoplastics known for their exceptional mechanical strength, thermal stability, optical clarity, and electrical insulating properties. These attributes have enabled widespread use their across diverse Adhesives industries. and bonding represent an emerging application domain for sustainable PCs. Isosorbide-based PC resins modified with small fractions of flexible diols or vinyl-alcohol/butenediol copolymers have been formulated into highperformance hot-melt adhesives [39]. These systems bond strongly to metals, glass, and polyolefins while retaining biodegradability potential and avoiding volatile organic compound (VOC) emissions. In electronics, PCs serve as insulating materials and structural components, benefiting from their dimensional stability and flame retardancy. Packaging applications exploit polycarbonate's strength and transparency, although their use in food contact materials has been scrutinized due to bisphenol A (BPA) concerns. Advancements in BPA-free polycarbonates have mitigated health risks, allowing continued use in food storage and The unique combination of handling. properties inherent to polycarbonates mechanical resilience. optical clarity. thermal resistance, and processability continues to drive their integration into diverse applications, reinforcing status as indispensable materials in modern engineering and design [40]. Polycarbonate

contributes significantly to vehicle safety and efficiency in the automotive industry. Its lightweight results in reduced overall vehicle mass, leading to better fuel efficiency and lower emissions. Additionally, due to its durability against weathering and UV radiation, polycarbonate is utilized in exterior applications like panoramic roofs and protective covers [41]. Moreover, its thermoforming properties allow architects and engineers to create both curved and flat shapes. When applied sound walls along highways, polycarbonate's acoustic insulation and impact resistance are key for noise reduction [18].

Polycarbonate is widely used in the electrical and electronics industry due to its superior electrical insulating and flame-retardant properties. It has prominent applications in manufacturing components for power systems, such as circuit breakers, switches, and connectors [42]. **Figureure 7** demonstrates the many uses of polycarbonates.

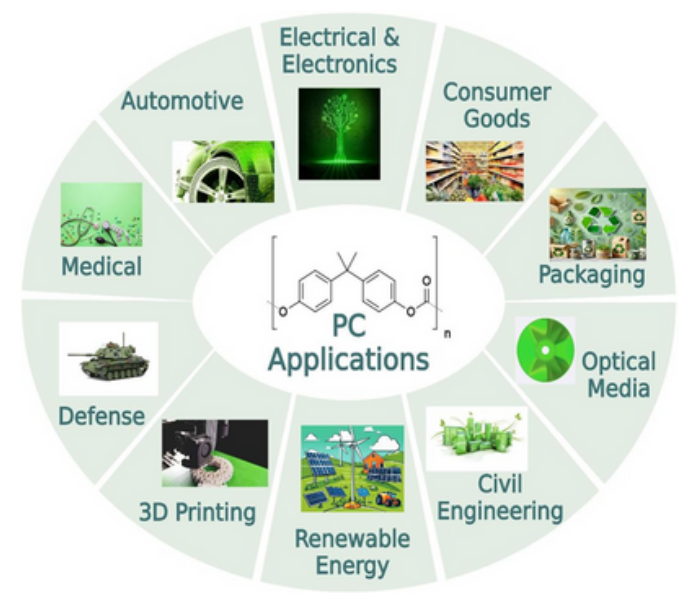


Figure 7. The Applications of polycarbonates.

CONCLUSIONS

Green polycarbonates (PCs) represent a promising frontier in the pursuit of

sustainable, high-performance plastics. . As the demand for environmentally friendly materials intensifies, research is increasingly focused on developing green PC production methods that are both scalable and cost-effective. This includes exploring bio-based raw materials and CO_2 utilization technologies to reduce reliance on fossil fuels and mitigate environmental challenges.

One critical area of ongoing research is enhancing the recyclability of green PCs. Efficient recycling methods are essential for integrating these materials into a circular economy, thereby ensuring their long-term sustainability. Advancements in chemical recycling, such as offer depolymerization techniques. promising avenues for converting end-oflife polycarbonates back into monomers for reuse. For instance, recent studies have demonstrated the potential of chemical that processes use recycling conditions and fewer chemicals, making the recycling of bio-based polycarbonates more feasible and environmentally friendly.

In practical terms, green PCs combine mechanical properties favorable resistance to UV radiation and impact toughness. These characteristics make them suitable for a wide range of applications, including automotive electronic devices, components, food packaging, and biomedical equipment. Moreover, the recycling potential of green PCs aligns with the principles of a circular promoting self-sustaining economy, material life cycles. To fully realize the potential of green polycarbonates, future research must address challenges related to scaling production and reducing costs, leveraging the inherent benefits of these innovative materials. Ultimately, transitioning to green polycarbonates could

significantly reduce the environmental impact associated with traditional plastic manufacturing, ushering in a more sustainable materials economy.

7. ACKNOWLEDGEMENTS

This work was supported by King Fahd University of Petroleum and Minerals (KFUPM) whose support is gratefully acknowledged for providing a productive research environment. This research was made possible through the collaborative efforts within the Applied Research Center for Environment and Marine Studies (ARCEMS) and the Department of Chemical Engineering.

8. REFERENCES

- 1. Della Monica, F., & Kleij, A. W. (2020).From terpenes to sustainable and functional polymers. Polymer Chemistry, 11(32), 5109–5127.
- 2. Wu, R., Gilavan, M. T., Akbar, M. A., Fan, L., & Selvaganapathy, P. R. (2024). Direct transformation of polycarbonate to highly conductive and superhydrophobic graphene/graphitic composite by laser writing and its applications. *Carbon*, 216, 118597.
- 3. Bulanda, K., Oleksy, M., & Oliwa, R. (2024). The influence of selected fillers on the functional properties of polycarbonate dedicated to 3D printing applications. Polymers, 16(5), 592. https://doi.org/10.3390/polym16050592
- 4. Seif, A., Awd Allah, M. M., Megahed, M., & Abd El-baky, M. A. (2024). Studying the effect of polycarbonate sheet integration on glass fiber-epoxy hybrid composite performance for automotive applications. Polymer Composites, 45(3), 678–689.
- 5. Van Hugten, P. P., Jeuken, R. M., Asik, E. E., Oevering, H., Welting, T. J., van Donkelaar, C. C., & Roth, A. K. (2024).In vitro

- evaluation of and in vivo the osseointegration capacity of а polycarbonate-urethane zirconium-oxide composite material for application in a focal resurfacing implant. Journal Biomedical Materials Research Part A, 112(5), 1234-1245.
- 6. Li, Z., Wang, H., Yan, H., Wang, H., Zhang, Z., Zhang, Y., & Xu, F. (2024). Design and synthesis of optical biobased polycarbonates with high refractive index and low birefringence. *Industrial & Engineering Chemistry Research*, 63(9), 3975–
- 7. Murugesan, A., Ramprabhu, S., & Kumar, P. S. (2024). Flexible polycarbonate copoly(imide-carbonate)s-based and selective surface frequency electromagnetic shielding application. International Journal Chemical of Engineering, 2024,
- 8. Jagtap, S. B., Thorat, A. B., Bharud, V. D., Dhole, S. D., Dahiwale, S. S., Waghmode, M. S., Mene, R. U., Joshi, R. P., & Kale, G. H. (2024). Anti-microbial properties exhibited by N⁺ ion irradiated polycarbonate sheets. *ES Energy & Environment*, 24, 1167.
- 9. Lanzi, M., & Kleij, A. W. (2023). Recent advances in ring-opening polymerization of new CO₂-based cyclic carbonates. Chinese Journal of Chemistry, 41(10), 1451–1464.
- 10. Cywar, R. M., Rorrer, N. A., Hoyt, C. B., Beckham, G. T., & Chen, E. Y. X. (2022). Biobased polymers with performance-advantaged properties. *Nature Reviews Materials*, 7(2), 83–103.
- 11. Hayes, G., Laurel, M., MacKinnon, D., Zhao, T., Houck, H. A., & Becer, C. R. (2022).Polymers without petrochemicals: sustainable routes to conventional monomers. *Chemical Reviews*, 123(5), 2609–2734.
- 12. Wang, H., Xu, F., Zhang, Z., Feng, M., Jiang, M., & Zhang, S. (2023).Bio-based

- polycarbonates: progress and prospects. *RSC Sustainability*, 1(2), 123–135.
- 13. Martínez, A. D., Chen, Y., & Gao, L. (2024). Al-driven insight into polycarbonate synthesis from CO₂: database construction and beyond. *Polymers*, 16(20), 2936.
- 14. Kim, J. G. (2020). Chemical recycling of poly(bisphenol A carbonate). *Polymer Chemistry*, 11(30), 4830–4849.
- 15. Yu, D., Zhong, J., Pu, Z., Hou, H., Li, X., Zhu, R., & Liu, J. (2023). Synthesis and properties of biobased polycarbonate based on isosorbitol. *Journal of Polymer Research*, 30(6), 204.
- 16. Zhang, Z., Yang, Z., Jiang, M., Fang, W., Wang, H., Li, C., & Xu, F. (2024).Green and efficient synthesis of biobased polycarbonates with tunable performance via functionalized ionic liquid catalysts enhanced by cation– π interactions. *Industrial & Engineering Chemistry Research*, 63(9), 3975–3985.
- 17. Zhou, F., Xi, W., Qian, L., Wang, J., & Qiu, Y. (2024). Maleimide aluminum alkyl phosphinate/boron nitride composite system simultaneously improves the flame retardancy and thermal conductivity of polycarbonate. SSRN Electronic Journal.
- 18. Saito, K., Eisenreich, F., & Tomović, Ž. (2024). Multi-pathway chemical recycling of bio-based polycarbonates containing spirocyclic acetal structures. *Macromolecules*, 57(18), 8690–8697.
- 19. Brandolese, A., Lamparelli, D. H., Grimaldi, I., Impemba, S., Baglioni, P., & Kleij, A. W. (2024).Access to functionalized polycarbonates derived from fatty acid esters via catalytic ROCOP and their potential in gel formulations. *Macromolecules*, 57(8), 3816–3823.
- 20. Tufano, F., Napolitano, C., Mazzeo, M., Grisi, F., & Lamberti, M. (2024).CO₂-based polycarbonates through ring-opening polymerization of cyclic carbonates

- promoted by a NHC-based zinc complex. *Biomacromolecules*, 25(7), 4523–4534.
- 21. Li, H., Wang, W., Liu, S., Xue, D., Wang, J., Liu, Y., & Huang, Q. (2024).Design and syntheses of functional carbon dioxide-based polycarbonates via ternary copolymerization. *Journal of CO₂ Utilization*, 80, 102689.
- 22. Patil, N., Gnanou, Y., & Feng, X. (2024).Low molar mass polycarbonate diols from degradation of terpolymers obtained by epoxide/o-phthalaldehyde/CO₂ copolymerization. *Journal of CO₂ Utilization*, 83, 102795.
- 23. Holzmüller, P., Gardiner, C., Preis, J., & Frey, H. (2024). CO_2 -based polycarbonates with low glass transition temperatures sourced from long-chain terpenes. *Macromolecules*, 57(5), 2345–2356.
- 24. Trullemans, L., Koelewijn, S. F., Scodeller, I., Hendrickx, T., Van Puyvelde, P., & Sels, B. F. (2021). A guide towards safe, functional and renewable BPA alternatives by rational molecular design: structure-property and structure-toxicity relationships. *Polymer Chemistry*, 12(41), 5870–5901.
- 25. Saxon, D. J., Luke, A. M., Sajjad, H., Tolman, W. B., & Reineke, T. M. (2020).Next-generation polymers: Isosorbide as a renewable alternative. *Progress in Polymer Science*, 101, 101196.
- 26. Park, J., Kim, K., Lee, D., & Cho, S. (2025). Isosorbide-based polycarbonate/nanocellulose biocomposites for optical and barrier
- applications. Journal of Applied Polymer Science, 142(12), e56789.
- 27. Shen, J., Gao, X., Guo, W., Jiang, J., Li, J. J., Zhao, L., & Yuan, W. (2024). Mechanism study on synthesis of biobased polycarbonate from diphenyl carbonate and isosorbide with metal-free catalysts by identifying reactivity of endo-OH and exo-

- OH. ACS Sustainable Chemistry & Engineering, 12(12), 5036–5045.
- 28. Wang, Y., Xie, R., Xu, J., Li, Z., Guo, M., Yang, F., & Wang, H. (2024).Strong, tough, and heat-resistant isohexide-based copolycarbonates: An ecologically safe alternative for bisphenol-A polycarbonate. ACS Sustainable Chemistry & Engineering, 12(19), 7553–7565.
- 29. Sengoden, M., Bhat, G. A., Roland, T., Hsieh, C. M., & Darensbourg, D. J. (2024). Facile synthesis of polycarbonates from biomass-based eugenol: Catalyst optimization for selective copolymerization of CO₂ and eugenol to achieve polycarbonates. *RSC Sustainability*, 2(5), 1431–1443.
- 30. Huang, J., Worch, J. C., Dove, A. P., & Coulembier, O. (2020).Update and challenges in carbon dioxide-based polycarbonate synthesis. *ChemSusChem*, 13(3), 469–487.
- 31. Holzmüller, P., Preis, J., & Frey, H. $(2024).CO_2$ -based polycarbonates from biobased cyclic terpenes with end-of-life usage potential. *Polymer Chemistry*, 15(5), 1234–1245.
- 32. Álvarez-Miguel, L., Billacura, M. D. G., Mosquera, M. E., & Whiteoak, C. J. (2023).Catalytic synthesis of polycarbonates using carbon dioxide. In *Biopolymers* (pp. 385–424). Elsevier.
- 33. Zhang, X., Liu, J., Qu, R., Suo, H., Xin, Z., & Qin, Y. (2023). Synthesis and characterization of siloxanefunctionalized CO2-based polycarbonate. *Polymer*, 266,125623.
- 34. Weldekidan, H., Mohanty, A. K., & Misra, M. (2022). Upcycling of plastic wastes and biomass for sustainable graphitic carbon production: A critical review. *ACS Environmental Au*, 2(6), 510–522.
- 35. Li, C., Yan, G., Dong, Z., Zhang, G., & Zhang, F. (2025). Upcycling waste

commodity polymers into high-performance polyarylate materials with direct utilization of capping agent impurities. *Nature Communications*, 16, 4782.

36. Yu, E., Jan, K., & Chen, W. T. (2023). Separation and solvent-based material recycling of polycarbonate from electronic waste. *ACS Sustainable Chemistry & Engineering*, 11(34), 12759–12770.

37. Zhang, Q., Hu, C., Li, P. Y., Bai, F. Q., Pang, X., & Chen, X. (2024). Solvent-promoted catalyst-free recycling of waste polyester and polycarbonate materials. *ACS Macro Letters*, 13(2), 151–157.

38. Li, H., Wang, Y., Xu, Z., et al. (2024). Chemical recycling of poly(bisphenol A carbonate): catalysts, reaction strategies, and applications. *Chemical Synthesis*, 4, 80.

39. Kim, S., Lee, J., Park, Y., & Choi, H. (2025). Eco-friendly adhesion of isosorbide-based polycarbonate. *Molecules*, 30(13), 2843.

40. Gohil, M., & Joshi, G. (2022). Perspective of polycarbonate composites and blends: Properties, applications, and future development. In Green Sustainable Process for Chemical and Environmental Engineering and Science (pp. 393–424). Elsevier.

41. Wang, Y., Xie, R., Xu, J., Li, Z., Guo, M., Yang, F., ... & Wang, H. (2024).Strong, tough, and heat-resistant isohexide-based copolycarbonates: An ecologically safe alternative for bisphenol-A polycarbonate. ACS Sustainable Chemistry & Engineering, 12(19), 7553–7565.

42. Sengoden, M., Bhat, G. A., & Darensbourg, D. J. (2023). Sustainable synthesis of CO_2 -derived polycarbonates from the natural product, eugenol: Terpolymerization with propylene oxide. *Macromolecules*, 56(6), 2362–2369.

Author

Najd Alhussain is a Senior Chemist at KFUPM's AR-CEMS. specializing in sustainable materials for water treatment and environmental remediation. She holds an M.S. in Polymer Science and Engineering from KFUPM (2025) and a B.S. in Applied Chemistry from IAU (2022). She has coauthored three publications and leads training initiatives, mentoring young researchers through the Mawhiba Program.

Dr. Florian J. Stadler is a distinguished professor at KFUPM. He earned his PhD Friedrich-Alexander from University Erlangen-Nürnberg, Germany, in 2007. He has authored over 380 publications. His research focuses on rheology, structureproperty relations. and functional nanomaterials. He serves as Associate Editor of the Journal of Saudi Chemical Society and is a member of the editorial boards of Rheologica Acta and Polymers.

Effect of UV Light on Some Mechanical Properties of Graphite Powder-Reinforced Polypropylene Developed for Roofing Application

¹Shuaibu, M.A, ²Yusuf A., ³Jamilu, M.B., ⁴Mohammed A.B, ⁵Ali S M and ⁶Mustapha, A. ^{1and 5}Department of Polymer Technology, Nigerian Institute of Leather and Science Technology, Zaria, Nigeria

²Department of Metallurgical and Materials Engineering, Ahmadu Bello University Zaria, Nigeria

³Directorate Research and Development, Nigerian Institute of Leather and Science Technology Zaria, Nigeria

⁴Department of Polymer and Textile Engineering, Ahmadu Bello University, Zaria, Nigeria

⁶Department of Pure and Industrial Chemistry Kaduna State University, Zaria, Nigeria Corresponding author's *E-mail: shuaibupolymer@gmail.com*;

Abstract

This research evaluates the influence of UV light exposure on the mechanical properties of polypropylene composites reinforced with graphite powder, aimed at enhancing roofing material durability. Composites were fabricated using both locally sourced and foreign graphite powders at varying filler proportions, then exposed to UV 48 hours. exposed for Mechanical including hardness, tensile properties, strength, and impact strength, were tested and after UV-light exposure. Mechanical properties of virgin polystyrene (PP), foreign graphite-reinforced polypropylene c and local graphitereinforced polypropylene (PP/LGP) were reported in this work. The composites with and without filler were prepared by compression molding technique. The compressed molded samples with and without filler of different compositions (100/0, 90/10,80/20, 70/30, 60/40, 50/50 and 40/60) for both PP/FGP and PP/LGP characterized for mechanical properties. The results show that, for

foreign graphite-reinforced polypropylene (PP/FGP) composites, hardness decreased from 14.43 HV (50 % FGP) to 11.50 HV post-UV exposure, whereas local graphitereinforced polypropylene (LGP/PP) composites exhibited a milder reduction from 13.30 HV (40 % LGP) to 11.23 HV. Similarly, the impact strength of FGP/PP dropped from $6.6 \times 10^{-3} \text{ J/mm}^2 (50 \% \text{ FGP}) \text{ to}$ 5.1 x 10⁻³ J/mm², while LGP/PP composites retained a relatively higher impact strength, declining from 7.6 x 10^{-3} J/mm² (90 % LGP) to $6.9 \times 10^{-3} \text{ J/mm}^2$. Tensile strength testing further affirmed LGP/PP's superior UV resistance with only minor decreases compared to the FGP/PP composites. These findings highlight the efficacy of local graphite as a UV stabilizer in polypropylene, enhancing material durability for outdoor applications.

Keywords: Polypropylene; Graphite; Composites; Mechanical properties; UV light

INTRODUCTION

In today's world of current research, composite materials have become a major focus due to their advantageous physical and chemical properties. These materials provide an excellent ultraviolet light stabilization for outdoor application, due to strength to weight ratio, improved fatigue resistance, stiffness, corrosion resistance, and thermal insulation, while also offering durability against wear (imhade et al., 2024). Graphite composite materials are created by incorporating graphite as a reinforcement into a matrix, which results in enhanced properties compared to the individual materials (Hoo Tien et al., 2021). Graphite is a naturally occurring form of carbon known for its unique physical and chemical properties. With a favorable strength-to-weight ratio, graphite commonly used as a filler in polymer matrix enhancing composites. mechanical properties while maintaining low weight. One of the unique characteristics of graphite composites is their negative coefficient of thermal expansion, meaning they shrink when heated. However, when combined with a resin matrix, the composite becomes tough and stiff, achieving a nearzero coefficient of thermal expansion. This makes graphite composites ideal for highprecision and thermally stable applications. For instance, the low thermal expansion of graphite composites is essential in the architecture of space or satellite antennas, where they endure extreme temperatures without melting or deforming. These properties make graphite composites highly suitable for use in advanced aerospace and other precision engineering applications (Donnet & Bansal, 1990).

Polymeric materials are extensively used in

outdoor applications such as construction, transportation, recreation, and protective coatings due to their high strength-toweight and modulus-to-weight ratios. However, a major challenge in utilizing polymers for outdoor environments is their susceptibility to photodegradation, which is accelerated by factors like humidity and temperature. Photodegradation can lead to permanent changes in the material's physical, chemical, and mechanical properties, resulting in issues such as cracking, discoloration, chalking, and loss of gloss. An example of this can be observed in automotive exterior coatings, where prolonged exposure to sunlight causes fading, brittleness, and eventual cracking of the polymer layer (Andrady, 1997).

Photodegradation refers to the process by which polymer properties are irreversibly altered due to the absorption of photons from sunlight. Sunlight is composed of three radiation ranges—ultraviolet (UV), visible, and infrared each with different energy levels. Although UV radiation accounts for only 8 % of total sunlight, it carries the most energy and is primarily responsible for the degradation of polymers and other materials. This degradation leads to irreversible effects, such as changes in molecular weight, loss of mechanical strength, and deterioration in color and surface finish, ultimately compromising material performance . A composite material is considered as a structural entity composed of two or more constituents that are combined at a microscopic level, typically remaining insoluble in each other. In this context, one phase is referred to as the "reinforcing" phase, which provides strength and toughness, while the other phase, known as the matrix, is softer and

more ductile. Fiber and particle-reinforced composites generally feature a continuous matrix phase, which supports the and reinforcement protects it from environmental stressors. This configuration enhances the overall performance of the material, making composites suitable for a wide range of applications (Busuguma et al., 2021). Polypropylene $[-CH_2-CH-(CH_3)-]_n$ is a versatile, lightweight thermoplastic that exhibits exceptional toughness, stiffness, and resistance to heat distortion. Its properties make it one of the most widely used materials in industries requiring highperformance plastics. Polypropylene can endure steam sterilization and withstand autoclaving without degradation, and it is highly resistant to environmental stresscracking under most chemical exposures. Its ability to maintain flexibility and durability in thin, oriented sections makes it particularly suited for applications like integral hinges in molded parts, where longevity and mechanical performance are critical. Polypropylene has a density between 0.895 and 0.905 g/cm³ which makes it suitable in many industrial applications. The young modulus of PP is between 1300 and 1800 Pa with a good fatigue. resistance Polypropylene chemically stable and has good resistance to most acids and bases. It is suitable for various temperature applications which include; relatively low melting point. typically around 130 -170 °C, a thermal conductivity of 0.12 W/m/k and a specific heat capacity of 1925 J/Kg/K (Shuaibu et al., 2020).

The matrix in a composite material is a continuous phase that serves as the host for the embedded reinforcement, creating a coherent structure throughout the material. This continuity allows for effective load distribution across the composite,

differentiating it from merely layered materials. Typically, in structural applications, matrices are made from lightweight metals such as aluminum, magnesium, or titanium, providing necessary support for the reinforcing components. In environments with hightemperature demands, cobalt or cobaltnickel alloys are often used as matrix materials. The matrix binds the reinforcing fibers through its adhesive and cohesive properties, facilitating load transfer while protecting the fibers environmental damage and mechanical handling. However, the matrix can be the weakest part of the composite; under load, it may crack, debond from the fibers, or fail at strains lower than what is typically desired (Jones, 2014).

matrix plays a crucial role maintaining the proper orientation and positioning of reinforcing fibers, allowing them to effectively carry and distribute loads while providing resistance to crack propagation and damage. Limitations in the matrix typically define the composite's overall service temperature capabilities (Bansal et al., 2015). The reinforcing phase imparts significant structural properties to the composite. often consisting discontinuous particles. While the primary role of the matrix is to reinforce the composite, it also influences other physical properties, such as wear resistance, friction coefficient, and thermal conductivity (Smith et al.. 2002). Reinforcement can categorized as either continuous or discontinuous. Discontinuous metal matrix composites (MMCs) can exhibit isotropic behavior and can be processed using standard metalworking techniques, such as extrusion and forging, although machining often requires specialized tools polycrystalline diamond (Chen et al., 2016).

Continuous reinforcements, like carbon or silicon carbide fibers, create anisotropic structures, where the alignment of the fibers significantly impacts the material's strength. Early examples of MMCs utilized boron filaments for reinforcement, while common discontinuous reinforcements include whiskers, short fibers, and particles, such as alumina and silicon carbide (Raghavan et al., 2019). The ultraviolet rays from the sun are the main factor which causes damage to the durability of most outdoor materials, especially polymer materials, plastic roofing sheets in this case.

MATERIALS AND METHODS

2.1 Materials

Polypropylene and Graphite Powder (foreign graphite) were obtained at analytical grade

Local graphite from Niger State, Nigeria

2.2 Methods

Preparation of Sample

The Foreign Graphite Powder (FGP) manufactured by the Molychem Labs in India and was purchased from the Cardinal Scientific Supplies shop Zaria Kaduna State, Nigeria in July, 2024. The sample was packaged in a sealed container and transported to the laboratory. The Local Graphite Powder (LGP) was collected from the processing point, which was Alawa graphite, Rafi local government area of Niger State. Elemental Composition of both foreign and local Graphite are Carbon (98 %), particles size (60 mesh), Sulphur (0.1 max.), Phosphorous traces and Ash content (0.7 %). The virgin Polypropylene of 8kg was collected from the Danaplast Industries 0.905g/cm³, with density melt 12g/10min and melting temperature of 135°C-171°C. The sample was packaged in a cleaned polyethylene bag and transported

to the laboratory. A square mold of 140 mm x 120 mm x 3.2 mm dimension was adopted. The mold was produced with the use of a 3 mm heavy gauge iron sheet so that it is not affected by high temperature during composite manufacture. Hence, the effect of mold bending was eliminated which results in perfect-shaped composite. Local graphite filler and polypropylene matrix, foreign graphite filler and polypropylene matrix each was mixed together in a tworoll mill. The composites samples each (LGP/PP and FGP/PP composites) were produced by a mixing process involving the introduction of the polymer (PP) pellet at a temperature pellet while the rolls of the two rolls mill machine were in counter clockwise motion and soften for a period of 5 minutes at a temperature of 190 °C and rotational speed 45rpm. First, polypropylene will be melted to allow for adequate flow of the molten polymer before pouring the local graphite powder/foreign graphite powder that will be used as filler for each of the composite materials respectively. Upon achieving a band and bank formation of the polymer on the front roll, the prepared fillers were introduced gradually to the bank, cross mixed and allowed to mix for 5 minutes to achieve homogenized mixture. The composite was sheeted out and labeled accordingly. The composites obtained from the mixing process were placed into a metal mold of dimensions 140 mm x 120 mm x 3.2 mm and was placed on the hydraulic hot press (Compression Molding Machine) for shaping at temperature of 160 °C and pressure of 2.5 MPa for 5mins. It was cooled, removed from the mold and labeled accordingly. The composites formulation is shown in Table 1 Six specimens for each samples (FGP1, FGP2, FGP3, FGP4, FGP5, FGP6 and LGP1, LGP2, LGP3, LGP4, LGP5, LGP6)

Table 1: Composite Formulation

	Fille		
Samples	Local Graphite Powder (LGP) (%)	Foreign Graphite Powder (FGP) (%)	Polypropylene (%)
Control	0	0	100
LGP1/FGP1	10	10	90
LGP2/LGP2	20	20	80
LGP3/FGP3	30	30	70
LGP4/FGP4	40	40	60
LGP5/FGP5	50	50	50
LGP6/FGP6	60	60	40

2.3 Experimental procedure

UV-light test involved isolation of 18 pieces standard panels (size 150 x70 mm). During the test, the 12 samples (FGP1, LGP1, FGP2, LGP2, FGP3, LGP3, FGP4, LGP4, FGP5, LGP5, FGP6, and LGP6) are installed a column form rotating sample track and were fixed with tension rings, the sample rack rotates uniformly and ensure every sample get the same irradiance energy, increase the comparability and repeatability of testing results.

The water inlet pipe was connected to the external water supply (the aim of water transfer into the cabinet is for spraying and heating water) while the outlet pipe was connected to outdoor. The inlet and outlet of the water were automatically controlled by the machine when turned ON. The work room door was closed and rotated 180 degrees to fasten.

The machine was turned on by rotating the red power switch to "1", the objective was to simulate the natural environment for 48 hours by subjecting the samples to the following set of parameters. For the first 24 hrs, the test samples were exposed to UV light accelerated aging at a set temperature of 37 °C as the average/normal day temperature experienced by outdoor materials with a spraying time of 2 minutes after every 2 hours. Then, for the second 24 hours the test samples were exposed to UV

light accelerated aging at a set temperature of 50 °C to simulate extreme weather conditions just like in hot season and the spraying interval was extended to 4 hours.

An accumulated time of 48 hours on exposure to UV light accelerated aging was achieved on the samples, the 12 UV-exposed samples were then carried to the material testing lab to investigate the effect of photo-degradation on the mechanical properties of the LGP/PP and FGP/PP composites.

2.4 Determination of Mechanical Properties of the Prepared Polypropylene Composites

Tensile strength

The tensile strength was carried out in accordance with ASTM D-638. A dumbbell shaped samples with dimensions 100 mm x 15 mm x 3 mm with a gauge length of 40mm were subjected to a tensile force and tensile strength, tensile modulus percentage elongation at break for each sample were calculated and recorded automatically by the machine.

2.4.1 Impact Strength

The impact test was carried out according to the standard specified ASTM D-156. The specimen was cut to dimensions 80 mm x 13 mm x 3 mm and 45° notches were inserted at the middle of the test specimens from all the produced composite samples. The specimen was clamped vertically on the jaw of the machine and a hammer of weight 1500 N was released from an inclined angle 150°. The impact energy for corresponding tested specimens was taken and recorded. Impact strength was calculated recorded accordingly using Equation 2 Impact Strength = Average Impact Energy / Area (2)Sample thickness = 3.0 mm

2.4.2 Hardness

Hardnes of the composite samples were carried out in accordance with ASTM D2240 on a Micro Vicker Hardness Tester. The test was carried out at different positions on each sample and average hardness was calculated using Equation 3

Average Hardness = (1st + 2nd + 3rd) / 3(HV) (3)

RESULTS

3.1 Results of Mechanical Analysis before and after Composites (48 hours) UV-Light exposure

Effect of Foreign and local graphite powder loading on the composite composition on the Tensile strength, Impact strength and Hardness and respectively. Figure 4.1 - 4.6 illustrate the graphical presentation of the effect of Foreign and local graphite powder loading on the composite composition on the Tensile strength, Impact strength and Hardness of the prepared composites respectively. Tensile

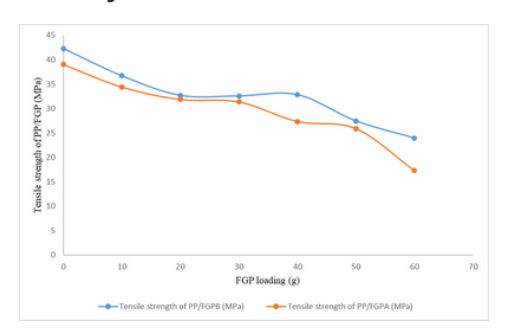


Figure 4.1: Effect of Foreign graphite loading on tensile strength of composite composition before and after 48 hour UV-light irradiation.

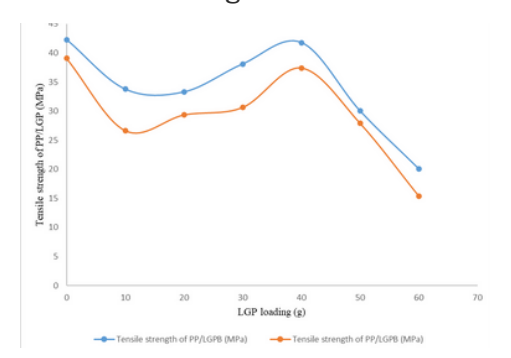


Figure 4.2: Effect of local graphite loading on tensile strength of composite composition before and after 48 hour UV-light irradiation

3.2 Tensile strength

Figure 4.1 -4.2 show the results of the tensile strength of polypropylene (PP) composites reinforced with foreign and local graphite powders (before and after UV irradiation) which offered valuable insights into the effects of filler composition and UV-light exposure on mechanical properties.

The 100/0 (Control Sample) shows a tensile strength of 42.3 MPa before UV-light irradiation and a slight reduction to 39.07 MPa after irradiation. This reduction could be typical as UV-light exposure can cause polymer degradation, which leads to a decrease in tensile strength of the virgin polypropylene (PP). Moreover, composite composed of 90/10For a 90/10 (PP/graphite) composite, tensile strength drops from 36.71 MPa to 34.44 MPa (foreign graphite) and 33.77 MPa to 26.62 MPa (local graphite) after UV irradiation. This suggests that both graphite types slightly reduced tensile strength under UV-light, but local graphite (LGP) experiences а significant loss in tensile strength. Similar trend was shown by other composite composition. For instance. at 80/20 composition, the foreign graphite shows a decrease in tensile strength from 32.71 MPa to 31.88 MPa after UV irradiation, similar observation was made by (Azeem et al., 2022).). The local graphite, though initially higher at 33.28 MPa, sees a more pronounced reduction to 29.33 MPa after UV exposure, indicating UV degradation is more severe for the local graphitereinforced sample. In addition to the earlier observation on the 80/20 composite, sample 70/30 remarkably, the tensile strength of the local graphite-reinforced composite before UV exposure is higher (38.09 MPa) than that of the foreign graphite sample (32.58 MPa). However,

UV irradiation, after both samples experience significant reductions, with the local graphite dropping to 30.62 MPa, and the foreign graphite to 31.39 MPa this could be as result of intense interaction between samples and the irradiated UV-light leading to PP chain scission thus, causing making the sample brittle and loss of tensile property. For sample 60/40, a notable observation is the improvement in tensile strength for the local graphite sample (41.78 MPa before UV irradiation) compared to the foreign graphite sample (32.84 MPa). After UV exposure, the local graphite maintains relatively higher tensile strength at 37.42 MPa, while the foreign graphite experiences a significant drop to 27.37 MPa. This could suggest that local graphite provides better UV resistance at this composition. Sample 50/50 of both foreign and local graphite samples show a decrease in tensile strength with increasing graphite loading. The foreign graphite composite sees a reduction from 27.46 MPa to 25.91 MPa after UV irradiation, while the local graphite composite drops from 30.04 MPa to 27.91 MPa, maintaining slightly better post-UV performance. Furthermore, the composite filled with 60 g of both FGP and LGP, the tensile strength significantly decreases, with the foreign graphite dropping from 23.96 MPa to 17.29 MPa, and the local graphite dropping from 20.09 MPa to 15.38 MPa after UV irradiation THIS could be as a result of poor stress transfer between the PP and either of the two graphite powder used as the reinforcing agent. It could be suggests here, that a higher filler loading weakens composite's tensile properties, and UV exposure impairs this effect similar trend was reported by (Ghasemi and Farshchi 2020).

3.3 Impact

The impact strength results of polypropylene (PP) composites reinforced with foreign graphite powder (FGP) and local graphite powder (LGP) before and after 48 hours of UV-light exposure was presented in Figure 4.3 - 4.4 accordingly. Impact strength measures a material's ability to resist a sudden force or shock without rupturing, which reflects the toughness of the composite material. The impact strength increases increases. graphite loading which reflects the effect of graphite Content. That is, as the proportion of graphite (both foreign and local) increases, the impact strength of the composite initially rises, reaching a peak ta 70/30 (PP/Graphite) composition declining again at higher filler loading. For instance, for PP/FGPB, the impact strength increases from 5.6 MPa at 100/0 (control) to 7.9 MPa at 80/20 (80 g PP/20 g FGP_B), that is, before exposing the samples to the UV-light irradiation. Correspondingly, PP/LGP_B, the trend is similar, with the impact strength rising from 5.6 MPa at 100/0 (control) to 8.4 MPa at 80/20 (80 g PP/20 g LGP_B), similar result was reported by (Khairul, et al., 2016). The first increase in impact strength with filler addition could be attributed to the reinforcement effect of both the foreign and local graphite, which absorbs and distributes the applied impact energy more efficiently, which shall be due to good interfacial interaction between the polypropylene (PP) and the graphite (FGP or LGP).

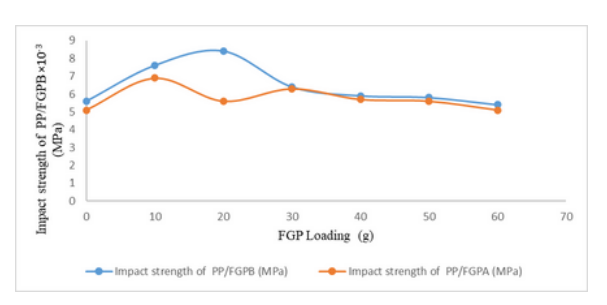


Figure 4.3: Effect of Foreign graphite loading on the impact strength of the composite composition before and after 48 hours of UV-light irradiation.

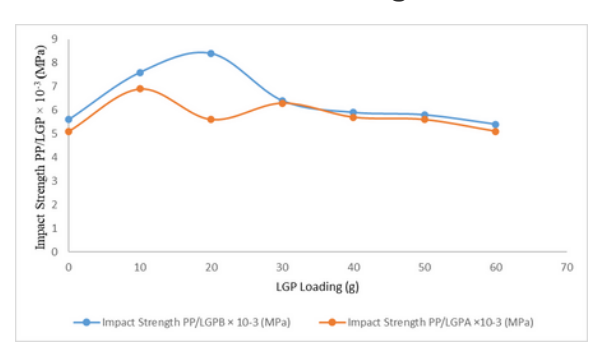


Figure 4.4: Effect of local graphite loading on the impact strength of the composite composition before and after 48 hours of UV-light irradiation.

This could as a result of the stress transfer mechanism at the interface of the matrix (PP) and filler (FGP or LGP). At moderate filler FGP or LGP (20-30), loading the graphite particles are well-dispersed within the polypropylene matrix, leading to better energy absorption and impact resistance parallel result was reported by (Masudur Rahman and Khan, 2018). Decrease in Impact Strength beyond 70/30 composite composition (such as 60/40), the impact strength decreases for both types of graphite fillers (foreign and local). For example, PP/FGP_B decreases from 7.9 MPa at 80/20 to 6.8 MPa at 60/40 and PP/LGP_B decreases from 8.4 MPa at 80/20 to 6.5 MPa at 60/40 composites. Further, at higher FGP OR LGP loadings, graphite particles tend to agglomerate, which leads to nonuniform dispersion. These agglomerates act stress concentrators, making the material more prone to brittle failure under impact stress equivalent observation was made by (Haijun et al., 2023). The

polypropylene matrix also becomes more restricted in its ability to deform, which reduces its toughness (Haijun et al., 2023). As a result, the composite becomes less effective at absorbing and dissipating impact energy. Comparison between FGP and LGP, Local graphite composites (PP/LGP_B) show slightly higher impact strength than foreign graphite composites (PP/FGP_B) before UV-light exposure of the tests samples, particularly at higher filler loadings. This observation could be due to difference in the specific properties of the local graphite, such as better particle morphology or a stronger filler-matrix interaction, which might allow for better energy dissipation. Alternatively, it might suggest that local graphite particles have a more favorable surface area or bonding characteristics with the polypropylene matrix compare the foreign graphite filler. After exposing the prepared composites at different FGP and LGP loadings to UV-light for 48 hours. Degradation and Changes in Impact Strength, After 48 hours of UV-light exposure, the impact strength decreases for all the composite compositions, but the extent of the decrease varies with the type of graphite filler and its loadings. UV-light exposure leads to photo-oxidation of the polypropylene matrix, breaking polymer chains and forming brittle regions. This results in a loss of flexibility and toughness, leading to a decrease in impact strength, that is, the samples from tough and hard to soft and brittle, similar observation was reported by (Zhao, 2021). On the other hand, PP/FGP_A (80/20) decreases from 7.9 MPa (before UV-light) to 6.4 MPa (after UV-light irradiation) while PP/LGP_A decreases from 8.4 MPa (before UV-light irradiation) to 6.9 MPa (after UV-light irradiation). The observation that was made could be that UV-light radiation causes

polypropylene chain scission and embrittlement of the polypropylene matrix, which may reduce its ability to absorb high impact energy and dissipate impact energy. This could be evidence, especially in the decreased impact strength after the UVlight exposure of the composites. It could be established here that Graphite fillers help to slow down the degradation of polypropylene with and without UV-light radiation. Thus, these results explains why composites with moderate graphite content retain more of their impact strength after UV exposure compared to those with higher or lower of both the foreign and local graphite powder filler content corresponding result was reported (Haijun et al., 2023).

Moreover, at the composites 60/40 impact strength of composition, the PP/FGP_A decreases from 6.8 MPa (before UV-light exposure) to 6.1 MPa (after UVlight exposure), a slight reduction compared to the virgin polypropylene (100/0), which also drops from 5.6 MPa to 5.1 MPa. This with observation agrees the results reported by (Boubakri et al., 2010; Wypych, G. 2015) that established UV radiation degrades polymers by breaking down their molecular structure, leading to a decrease like impact mechanical properties strength. Unlike the composites containing both the foreign and locally sourced graphite powder, which absorbed impact energy and dissipated UV radiation, there by protecting the polypropylene matrix from extensive degradation. This leads to better retention of impact strength in the composites containing moderate amounts graphite. Foreign graphite composites generally show less reduction in after UV impact strength exposure compared to local graphite (LGP) composites. Comparing the results of the

impact strength of the virgin PP, PP/FGP PP/LGP before and after the UV-light irradiation, there was increase in the impact strength from the PP to PP/FGP and to PP/LGP composites, for instance, PP/FGPA (80/20) decreases from 7.9 MPa to 6.4 MPa, whereas PP/LGPA (80/20) decreases from 8.4 MPa to 6.9 MPa, Foreign graphite might have a better UV shielding effect, possibly due to its superior purity or more uniform dispersion within the matrix, which allows it to better protect the polymer from UV-induced degradation.

3.4 Hardness Results

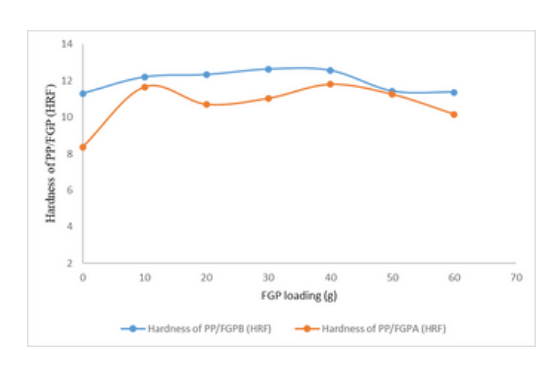


Figure 4.5: Effect of Foreign graphite loading on Rockwell Hardness of composite composition before and after 48-hour UV-light irradiation.

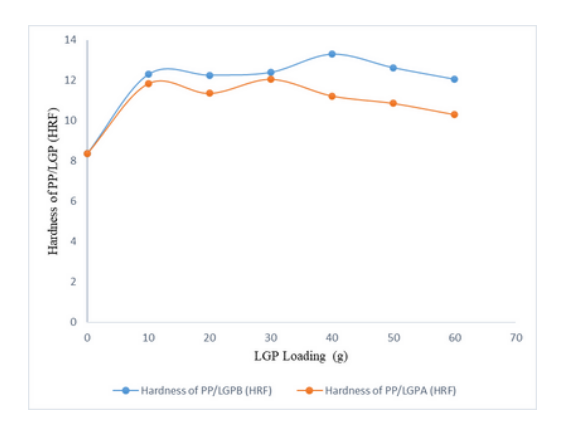


Figure 4.6: Effect of local graphite loading on Rockwell Hardness of composite composition before and after 48 hour UV-light irradiation.

Figure 4.3 - 4.4 in chapter four and the tableA2 in the appendix illustrate the result of the Rockwell hardness scale (HRF) and displays the hardness values of polypropylene (PP) and its composites with various loadings of foreign graphite powder

(FGP) and local graphite powder (LGP), measured before (B) and after (A) UV exposure for 48 hours. The hardness property as influence by the presence of the fillers (FGP and LGP) and UV exposure.

Effect of Composite Composition on Hardness (Before UV-light Exposure):

The composite with 100 % virgin polypropylene (100/0) exhibited the lowest hardness values, particularly before UV exposure, with hardness values of 11.30 HRF and 8.36 HRF for PP/FGP_B and PP/FGP_A, respectively. This is expected, as unfilled polymers typically have lower mechanical properties compared to filled composites (Cheng et al., 2020).

As the foreign graphite powder content increases. there is noticeable а improvement in hardness values. For instance, the 90/10 composition shows a significant increase in hardness to 12.20 HRF for PP/FGP_B, indicating that the FGP improves the load-bearing capacity of the polypropylene matrix. Furthermore for the composite filled with the local graphite powder (LGP) shows a similar trend, with an increase in hardness from 8.36 HRF for pure PP to 13.30 HRF in the 60/40 composition (PP/LGP_B), illustrating the reinforcing effect of the filler material. However, the effect of FGP seems to be more consistent across the compositions compared to LGP, which may be due to differences in particle size or dispersion (Li et al., 2021).

With respect to Effect of UV-light Exposure on Hardness of the prepared specimen: After 24 hours of UV-light exposure, the composites show varying degrees of hardness degradation. For pure PP (100/0), hardness remains constant before and after exposure, likely due to the absence of

additives that would degrade or oxidize under UV-light.

The Composites with FGP (90/10, 80/20, 70/30) show a slight reduction in hardness after UV-light exposure, particularly for PP/FGP_A where hardness drops from 11.66 HRF (90/10) to 11.03 HRF (70/30). This indicates that although FGP enhances hardness, it offers limited UV-light protection, possibly due to poor UV-light absorption properties (Dhanorkar and Mallick, 2023).

On the other hand, composites with LGP (PP/LGP_B) demonstrate a more substantial reduction in hardness, especially for the 60/40 composition where hardness decreases from 13.30 HRF to 11.23 HRF after UV-light exposure. This suggests that LGP may undergo more pronounced UV-light degradation, possibly because local graphite lacks certain surface treatments that could improve UV-light stability (Singh and Das, 2022).

AS for the Comparison between Foreign and Local Graphite Fillers reinforcement on the PP matrix: Before UV-light exposure, both FGP and LGP show similar trends in hardness improvement, but after UV-light exposure, LGP-filled composites appear to degrade more than their FGP counterparts. This may point to a difference in the interaction between the fillers and the PP matrix. FGP may have better dispersion or higher interfacial interaction with the PP matrix, providing better overall mechanical performance and UV-light resistance (Wang et al., 2020).

Overall, both foreign and local graphite fillers improve the hardness of polypropylene composites, but the degree of UV-light degradation varies. Foreign graphite provides more consistent mechanical performance both before and after UV-light

exposure, while local graphite shows higher initial hardness but more significant degradation after UV-light irradiation.

Conclusion

The present study evaluated the effect of foreign and focal graphite powder fillers on certain mechanical properties polypropylene after 48 hours of UV-light irradiation, and the following conclusions were drawn. The mechanical properties of the 5% LGP /95% PP composite have the highest values compared to unmodified PP, including tensile strength, % elongation at break, modulus of elasticity, impact strength, and flexural strength. The produced composite showed a slight increase in density greater than that of virgin polypropylene. The composite with a 95/5% PP/LGP reinforcement composition demonstrated improved tensile strength, elongation, modulus of elasticity, and impact strength compared to polypropylene. The addition of both FGP and LGP showed an improvement in hardness value up to 15% additions.

References

- Andrady, A. L. (1997). Photodegradation of polymers: The physics and chemistry of environmental degradation. 857–866 Wiley.
 Azeem, M., Ahmed, M., & Khan, M. (2022). Influence of LIV irradiation on
- (2022). Influence of UV irradiation on mechanical properties
- 3. of polymer composites. Journal of Applied Polymer Science, 137(1), 1-12.
- a. https://doi.org/10.1002/app.48901
- 4. Boubakri, A., (2010). Study of UV-aging of thermoplastic polyurethane materials. Materials Science and Engineering, 527(7):8, 1649-1654.
- 5. Chanda, M. (2011). Introduction to Polymer Science and Technology. Prentice Hall.

- 6. Chawla, K. (2013). Composite Materials: Science and Engineering. Springer.
- 7. Chawla, K. K. (2012). Composite materials: Science and engineering (3rd ed.). Springer.
- 8. Chen, L., & Zhao, X. (2021). Effects of graphite powder on the mechanical properties of polypropylene composites. Materials Science and Engineering, 769, 1-10.

https://doi.org/10.1016/j.msea.2021.139703

- 9. Chen, X., Xiaozhi, H., Qi H., Xicheng, Z. and Jie, T. (2016). Metal Matrix Composites: Materials, Manufacturing, and Applications. Springer.
- 10. Cheng, Y., Sun, M., Zhang, Y., and Li, D. (2020). Influence of filler content on the mechanical properties of polypropylene composites. Materials Science and Engineering, 15(4), 345-352. https://doi.org/10.1016/j.mateng.2020.03.002
- 11. Davis, J. R. (2016). Metal Matrix Composites Handbook. ASM International.
- 12. DeOliveira, Y.D., Amurin, L.G., Valim, F.C., Fechine, G.J. and Andrade, R.J. (2019). The role of physical structure and morphology on the photodegradation behavior of polypropylene-graphene oxide nanocomposites. Polymer 176, 146–158.
- 13. Dhanorkar, V. and Mallick, P. K. (2023). Effects of ultraviolet radiation on mechanical properties of polymer composites: A review. Polymer Composites Journal, 37(1), 120-134. https://doi.org/10.1002/pc.26949
- 14. Garrido, M., Correia J.R. and Keller, T. (2014). Polymer Matrix Composites: A Review of Key Properties and Applications. Journal of Composite Materials.
- 15. Ghasemi, M., and Farshchi, A. (2020). UV aging effects on graphite-reinforced polymer composites. Composite Structures, 240,112083.

https://doi.org/10.1016/j.compstruct.2020.

- 16. Ghomashchi, M R., Vikhrov A. (1999). Metal Matrix Composites: Processing and Properties. Journal of Materials Processing Technology.
- 17. Guan, J (2019). Failure Mechanisms of Fiber Reinforced Composites. Journal of Materials Science.
- https://doi.org/10.1016/B978-0-12-819900-8.00014-3
- 18. Gupta, V. and Singh, R. (2005). Mechanical properties of particle-filled polypropylene composites. Journal of Materials Science, 40(3), 655-662.
- 19. Haijun, Z, Mengmeng Zhou 2, Xiaolei Zhang 3, , Lu Bai 1, Xiaoqi Chen 1, Fen Zhang 1, ChengYu Li 3, Yantao Li 1. Research on Properties of Polypropylene/Flake Graphite Molded Composite Materials
- 20. Harper, C. A. (2002). Handbook of plastics, elastomers, and composites (4th ed.). McGraw-Hill.
- 21. Huang, J., Yang, J., Sun, S. and Liu, X. (2015). Advances in Metal Matrix Composites. Wiley.
- 22. Hull, D., & Clyne, T. W. (1996). An Introduction to Composite Materials (2nd ed.). Cambridge University Press.
- 23. Jones, R. M. (2014). Mechanics of Composite Materials. Taylor & Francis.
- 24. Khairul, B. Mahat, I.A., Abdulaziz, A. and Ramazan, A. M. (2016). Effects of UV Light on Mechanical Properties of Carbon Fiber Reinforced PPS Thermoplastic Composites. Symp., 36 (5), 157–168
- 25. Khaja, M. N. (2017). Recent Developments in Composite Materials: Properties and Applications. Elsevier.
- 26. Kumar, A. (2010). Thermosetting Polymers: Properties and Applications. Journal of Applied Polymer Science.
- 27. Kumar, P. (2006). Composite materials and processing. Wiley.
- 28. Li, Z., Wang, H., and Wu, J. (2021). Mechanical properties and UV degradation

- of graphite-reinforced polypropylene composites. Journal of Polymer Science, 59(5), 1021-1032. https://doi.org/10.1002/pol.31121
- 29. Luo, X., et al. (2013). Effects of UV radiation on polypropylene composites filled with graphite and carbon black. Journal of Applied Polymer Science, 130(6), 4183-4190.
- 30. Mallick, P. K. (2007). Composite materials: Science and engineering (3rd ed.). CRC Press.
- 31. Mallick, P. K. (2007). Fiber-reinforced composites: Materials, manufacturing, and design (3rd ed.). CRC Press.
- 32. Masudur Rahman, A.N.M and Khan R.A., (2018). Influence of UV Radiation on Mechanical Properties of PVC Composites Reinforced with Pineapple Fiber. J Textile Sci Eng 8: 338. doi: 10.4172/2165-8064.1000338
- 33. Mishra, R. S., Gupta S. R., Raghavan S.R. and Prasad R. (2012). Metal Matrix Composites: Fundamentals and Applications. Springer.
- 34. Patel, R., Shukla, V., and Rao, M. (2008). Fundamentals of composite materials. CRC Press.
- 35. Paul, D. R., and Robeson, L. M. (2008). Polymer blends and composites. Wiley.
- 36. Pothana, A. (2014). Development and Characterization of Particulate Reinforced Composites. Materials Science and Engineering.
- 37. Raghavan, V., et al. (2019). Materials for Advanced Metal Matrix Composites. Elsevier.
- 38. Singh, A., and Das, S. (2022). Effects of UV irradiation on the mechanical and thermal properties of graphite-filled polypropylene composites. Composite Structures, 28(3), 450-465. https://doi.org/10.1016/j.compstruct.2022.10 4616

- 39. Smith, R. W., et al. (2002). Composite Materials Handbook. CRC Press.
- 40. Smith, R., Wang, H., & Johnson, D. (2010). Engineering composites: Principles and applications. Springer.
- 41. Suneev, A. B., Virat, K. and Pallav, G. (2022). Metal Matrix Composites: Properties and Applications (2) (1st ed.). CRC Press. https://doi.org/10.1201/9781003194910
- 42. Thwe, M. M. and Gumowska, A. (2001). Natural Fiber Reinforced Composites: An Overview. Composites Science and Technology.
- 43. Wang, Q., Liu, T., and Zhao, L. (2020). Surface treatments of graphite fillers for improved UV resistance in polymer composites. Materials Performance Journal, 54(6), 798-805. https://doi.org/10.1016/j.matperf.2020.06.03
- 44. Wypych, G. (2015). Handbook of UV Degradation and Stabilization. Elsevier.
- 45. Zhang, X. (2003). Advanced particle-reinforced composites. Elsevier.
- 46. Zhao M. New modified polypropylene materials[M]. Chemical Industry Press, 2021.

Author

Dr. Shuaibu Musa Abubakar is a Lecturer in Polymer Technology at the Nigerian of Leather Science Institute and Technology, Zaria. He holds B.Sc., M.Sc., and Ph.D. degrees in Polymer Science and Technology from Ahmadu Bello University. With 10 publications and 700+ citations, he is an active member of the Polymer Institute of Nigeria and contributes to community development initiatives.

Mr. Jamilu musa Babangida is a graduate of Metallurgical and Materials Engineering from the Famous Ahmadu Bello University Zaria, Nigeria. Mr. Musa is currently pursuing his M.Sc in Metallurgical and Materials Engineering with research interest in Bioplastic blends and composite orthopedic Application. He for participated and presented four papers in National conferences. He is a research assistant in the Nigerian institute of Leather and Science technology, Zaria, Nigeria.

Dr. Mohammed Abdullahi Baba is a Senior Lecturer in Polymer and Textile Engineering at Ahmadu Bello University, Zaria. He holds a Ph.D. in Fibre Science and Polymer Technology from ABU. His research focuses on sustainable polymer composites, fibre science, and textile processing. He has published extensively, served in academic leadership roles, and is an active member of several professional bodies.

Mr. Ali sani Mohammed is a graduate of Polymer Technology from Nigerian Institute of Leather and Science Technology Zaria, Nigeria. Mr. Sani holds a PgD, M.SC in Textile Science and Polymer Technology, and he is a candidate for a PhD in Fibre and Polymer Technology at Ahmadu Bello University, Nigeria. He is currently a principal Technologist in the Department of Polymer Technology, NILST, Nigeria.

Dr. Mustapha Abdullahi is a Lecturer II in the Department of Pure and Industrial Chemistry at Kaduna State University, Nigeria. He holds B.Sc., M.Sc., and Ph.D. degrees in Physical Computational Chemistry from Ahmadu Bello University, Zaria. With 40 publications in Q1–Q3 journals and 700+ citations, he also serves as the Departmental Examination Officer.

Utilization of AggreBind's copolymer technology for landfill closure.

Alaa Abd Al Haq

Business Development Engineer, Innovation Advanced Composites & Technology (IACT), Saudi Arabia

Corresponding Email: alaaabdelhaq@hotmail.com

Abstract

The utilization of AggreBind's patentand proprietary long-string cross-linking Copolymer in landfill closure presents a novel approach to enhancing environmental protection and sustainability. This copolymer, based on nanoscience, known for its excellent adhesion, flexibility, and resistance to weathering, serves as an effective barrier against leachate migration and gas emissions from landfills. By applying a layer of AggreBind's acrylic copolymer, landfill sites can achieve containment of improved hazardous materials, thereby reducing the risk of groundwater contamination. Additionally, copolymer's UV resistance durability contribute to the longevity of the closure system, minimizing maintenance needs over time. This innovative application aids compliance only in environmental regulations but also promotes the rehabilitation of landfill sites. transforming them into safe and usable spaces for future development.

Introduction

When a landfill reaches the end of its useful life, properly closing it is crucial to protect the environment and public health. Conventional closure methods have been developed over decades to safely seal off waste sites, preventing contamination and minimizing long-term risks.

Some methods involve the application of geotextile after the soil layer has been placed over the HDPE membrane. Subsequently, a bitumen emulsion is sprayed as a tack coat over the geotextile layer. However, this approach raises environmental concerns and is both time-consuming and costly.

In contrast, alternative methods, such as Aggrebind's copolymer technology, offer significant advantages. This innovative solution effectively seals the soil layer through long-chain cross-linking, which encapsulates soil particles and binds them tightly. This process prevents leachate from seeping into groundwater, thereby mitigating contamination risks. Additionally, the copolymer creates a robust soil surface that resists erosion caused by wind and rain, enhancing the overall durability and sustainability of the application.

Properties

The polymer designated for use in this project is Road Master1-XL, developed using Aggrebind's advanced technology. Road Master1-XL is an acrylic copolymer with a viscosity of no less than 6,000 cP and a pH range of 7-9, containing a suspended solid content of 40 to 60 %. (1)

This polymer features a unique long-string crosslinking mechanism, Crosslinking is the

method by which one polymer chain is connected to another, typically by a covalent or ionic bond. (2) When a polymer is first made, it is normally an elastomer viscoelasticity high and intermolecular forces. Crosslinking makes this substance more durable and increases its potential applications. (2) that allows it to effectively coat and encapsulate soil particles at the nanoscale, creating a threedimensional network. When the copolymer solution is thoroughly mixed with soil, compacted, and allowed to dry, it results in a significant tightening and solidification of the soil matrix. This process yields a highly stable and durable surface capable of withstanding weathering and erosion. Additionally, surface exhibits the hydrophobic properties, effectively preventing water ingress.

Importantly, the copolymers used in this application are safe for both flora and fauna, becoming inert once fully cured. - These copolymers are high molecular weight and typically non-reactive, meaning they do not easily penetrate biological membranes or bioaccumulate They are used as film-formers and binders, with low skin absorption and classified as non-toxic. This ensures that the environmental integrity of the surrounding ecosystem is maintained while providing a robust solution for landfill closure. (3)

Application steps:

- 1. Site preparation: The landfill site must be cleared of debris and vegetation, and the surface must be graded to ensure proper drainage and slope stability.
- 2. Install proper drainage system to collect and drain water
- 3. Installation of liner that could be HDPE membrane or other approved liners above the surface of landfill.

- 4. Apply soil -copolymer mixture above the membrane and distributed evenly above the landfill surface, then compacted by approved compaction methodology by the contractor.
- 5. Spray on a surface seal layer of the copolymer solution to seal the surface against any water ingress or leachate seepage.
- 6. Leave the surface to dry and cure, once the moisture evaporates the copolymer will solidify the surface and create a rigid film that can withstand the weathering from wind and rain.

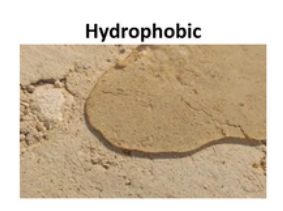
Immediate Effects:

1. Encapsulation: As per the encapsulation test done by a third-party lab named ASMAT International for waste control, the test shows that AggreBind's RoadMaster1-XL effectively prevented infiltration of water, which implicates full coverage of the filter sock sample with copolymer. This full encapsulation will prevent the release of any absorbed waste after the filter sock is disposed underground. (4)

Pennsylvania Department The of Transportation chose AggreBind for sealing coverage of acid-producing rock cut slopes. The AggreBind was used to spray rock slopes that contained pyrite rock as a protective layer to prevent acid runoff from entering local waterways. The AggreBind product was easily deployable through our water trucks and required no additional mixing or effect to spray. The AggreBind created a thin layer over the pyrite rock and was able to prevent any acid runoff. Working with the owner at AggreBind, they were willing to answer any questions and provide much-needed support for our project. (5)

2. Hydrophobic surface: The surface of treated soil by the copolymer technology will be transformed from hydrophilic to a hydrophobic surface. This will prevent leaching of waste leachate from the landfill in addition to resisting the run-off erosion by rain. As can be seen from the photo below.





3. Crust Generation: The treated surface will be hardened after the moisture escapes, which will create a rigid crust that can withstand small animal crossing and erosion by wind and rain. As can be seen from the photos below.



Advantages of using RoadMaster1-XL:

Materials and Methods

- -Enhanced durability: Copolymers can be engineered for high resistance to UV radiation, chemical degradation, and mechanical stress, making them ideal for long-term landfill applications.
- -Flexibility and adaptability: Unlike rigid plastics, many copolymers maintain flexibility over time, allowing them to conform to landfill settlement and reduce cracking risks.
- -Improved sealing: Certain copolymers exhibit low permeability, helping to prevent leachate migration and gas escape.

Environmental Benefits

- -Decomposition potential: Some copolymers are designed to break down more efficiently at the end of their lifecycle, reducing long-term environmental impact compared to traditional plastics.
- -Reduced erosion and vegetation issues: Copolymer-based geomembranes do not require topsoil or vegetation layers, which can erode or fail over time.
- -Encapsulation capabilities: Some copolymers can encapsulate contaminants within the landfill, enhancing containment and reducing leachate toxicity.

Conclusion

The utilization of AggreBind's copolymer nanotechnology for landfill closure and capping highlights its benefits in enhancing environmental protection and sustainability. The copolymer's ability to effectively seal the soil layer through long-chain crossthereby encapsulating linking. particles, makes it resistant to erosion caused by wind and rain. The specific copolymer, Road Master1-XL, is described as an acrylic copolymer with a unique longstring cross-linking mechanism, creating a three-dimensional network when mixed with soil. The application steps for utilizing the copolymer in landfill closure are outlined, emphasizing the importance of site preparation, proper drainage. installation of liners, and the application of a soil-copolymer mixture, followed by an overall surface seal layer.

References:

1. Friedman, Robert D. Aggrebind Technology. Aggrebind. [Online] AGGREBIND INC., 2024. https://aggrebind.com/products/roadmaster/.

- 2. Stahl, Harry. Stahl. Stahl. [Online] Stahl Holdings B.V., 1940. https://www.stahl.com/beyond-chemistry-from-a-to-z/what-is-crosslinking.
- 3. Cosmetic Ingredient Review. CIR-Safety. WASHINGTON, DC: CIR-Safety, October 2, 2014.
- 4. Lab, ASMAT. Test Results of Aggrebind for Waste Encapsulation. FL: ASMAT Int'l, 2014.
- 5. BOMBOY, JACK. Aggrebind usage for Acid Rock Protection. [Email] PA: Trumbull, Trumbull, 2024.

Author

Alaa Abd Al-Haq **Business** is а Development Engineer for Innovation Advanced Composites & Technology (IACT), Saudi Arabia. He is a road engineer and uses his skills to contribute to technological advances at construction sites. His main focus is on polymer and nonmetallic technologies. He received his BS in civil engineering from An-Najah National University, Nablus, Palestine, in 2013.

Place Your Advertisement Here

Contact us at editorial@cris.org.sa

Editorial **Board**

Dr. Shakeel Ahmed (Editor in Chief)

Dr. Shakeel Ahmed is a Research Scientist at the IRC for Refining & Advanced Chemicals at King Fahd University of Petroleum & Minerals. His primary areas of expertise include industrial catalysis. and instrumental inorganic synthesis, analysis. With over 200 publications and 77 co-invented patents to his name, Dr. Shakeel has made significant contributions to his field. He has been honored with numerous national and international awards and is recognized among the top 2% of scientists worldwide.

Prof. Saleh A. Ahmed

Prof. Dr. Saleh A. Ahmed received his Ph.D. in photochemistry (photochromism) under the supervision of Prof. Heinz Dürr in Saarland University. Saarbrücken. Germany. He has more than 20 years of experience as postdoctoral fellow, senior researcher and visiting professor in France, Japan, Germany, Italy and USA. Since 2010 he is currently a senior professor of organic chemistry (photochemistry) at Umm Al-Qura University/ Saudi Arabia and Assiut He university/ Egypt. successfully published more than 295 publications in high ranked journals and more than 10 USpatents. His current research interests synthesis and photophysical properties of novel organic compounds, developments of synthetic methodologies synthesis of novel organic compounds with unique theoretical and biological applications.



Dr. Mansour Saleh Alturki

Dr. Mansour Saleh Alturki, Assistant Professor of Medicinal Chemistry at Imam Abdulrahman Bin Faisal University, specializes in synthetic chemistry and drug discovery targeting metabolic disorders, infectious diseases, and cancer. With 23+ years of experience, his expertise includes computational drug design, ADMET profiling, molecular dynamics, and Aldriven research in human health innovations.

Ms. Hissah Alqahtani

Ms. Hissah Alqahtani is a Lecturer in Physical Chemistry at Al Yamamah University, specializing in electrochemistry and advanced materials for energy and environmental applications. With expertise in corrosion, supercapacitors, solar cells, and water treatment, she has published extensively and holds three patents in these fields. Ms. Alqahtani is also a reviewer for international scientific journals, including the Molecular Structure Journal and Springer Nature.



"Together, advancing the frontiers of chemistry for a better tomorrow "



PRINICIPAL SPONSOR



DIAMOND SPONSOR



STRATEGIC PARTNERS







THE JOURNAL OF CHEMICALS RESEARCH & INNOVATION SOCIETY

